# NATIONAL ADVISORY COMMITTEE FOR AERONAUTICS

TECHNICAL NOTE

No. 1324

## INTERACTION BETWEEN THE SPARS OF SEMIMONOCOQUE WINGS WITH CUTOUTS

By N. J. Hoff, Harry Kase, and Harold Liebowitz
Polytechnic Institute of Brooklyn





Washington
July 1947

NATIONAL ADVISORY COMMITTEE FOR AERONAUTICS

TECHNICAL NOTE NO. 1324

# INTERACTION BETWEEN THE SPARS OF SEMIMONOCOQUE WINGS WITH CUTOUTS

By N. J. Hoff, Harry Kase, and Harold Liebowitz

## SUMMARY

The stresses in the two spars of a model of a wing having three rectangular cutouts were calculated by the PIBAL method, a modification of Southwell's method of systematic relaxations. The model was built and tested in the Polytechnic Institute of Brooklyn Aeronautical Laboratories and the deflections and strains measured were compared with calculated values. The agreement was found to be satisfactory.

## INTRODUCTION

Many modern airplane wings are built with two spars rather than according to the true monocoque principle. Spars are provided because the full utilization for load-carrying purposes of the skin and its reinforcements is not possible when there are many cutouts for retracting landing gear, wing tanks, armament, and so forth near the root. The calculation of the interaction between the spars is a difficult task if the rigorous methods of the theory of elasticity are used. To disregard it, however, is wasteful since the ribs and the skin provide a comparatively strong elastic connection between the spars which relieves the more highly loaded spar at the expense of the less highly loaded one. The interaction between the spars of fabric-covered wooden wings was investigated by many authors. The earliest attempt appears to be contained in a paper by L. Ballenstedt (reference 1) published in 1918, while in the late twenties Th. von Kármán's group at Aachen developed and verified a rigorous and comparatively simple method of calculation (references 2 and 3). In England, D. Williams and H. Roxbee Cox worked out an interesting solution in 1933 (reference 4). All these papers dealt with wing structures without a load-carrying skin since at the time of their publication stressed-skin wings were seldom if ever used. However, in 1935 Paul Kuhn showed that the Friedrichs-Kármán equations can also be applied to the interaction problem of the more modern types of wing (reference 5). More recently, a theoretical solution was given

by W. J. Goodey, who used strain-energy methods in his analysis (reference 6).

The writers believe that there is a need for a procedure which can take into account variable cross sections, stressed skin, and cut-outs, and at the same time is simple enough to be used by little-trained personnel. It appears that the PIBAL method developed in reference 7 for the calculation of the stresses in reinforced flat and curved panels, rings and frames, and reinforced monocoque cylinders is well suited for the solution of the interaction problem with an accuracy sufficient for engineering purposes. It is based on the Southwell relaxation method (reference 8). The structure is assumed to be composed of several beam elements having bending, shearing, and torsional rigidity determined from the geometry of the wing structure and the mechanical properties of its materials of construction. The forces and moments corresponding to prescribed displacements of the end points of these elements are determined, and the conditions of equilibrium at these points are expressed in terms of the displacements. The result is a system of linear equations which in the present report is solved by matrix methods. In the Southwell method a solution is obtained by a systematic procedure of step-by-step approximations. The solution yields the displacements at the end points of the elements from which the stresses in any part of the structure can be easily calculated.

The results of the calculations were checked by experiments carried out with a model of a two-spar wing under various conditions of loading and end fixation. The agreement was found to be satisfactory.

The authors are much indebted to Dr. Bruno A. Boley and Mr. Bertram Klein for their advice and help during the construction and testing of the specimen and in the calculations, to Edo Aircraft Corporation, and to Mr. R. Ries of Edo Aircraft Corporation for contributing the formed rib flanges. The investigation was sponsored by and conducted with the financial assistance of the National Advisory Committee for Aeronautics.

## SYMBOLS

| | |
|---|---|
| $A$ | cross-sectional area of upper or lower flange |
| $A_c$ | cross-sectional area of compression flange |
| $A_i$ | area included by the thin wall of a closed section |
| $A_s$, $A_t$ | cross-sectional area of uprights, of tension flange |

| | |
|---|---|
| $A_x$, $A'$ | area of cross section of an interspar element |
| AB, BA, BB, 33, 35, etc. | subscripts used with influence coefficients, in which the first letter or number refers to the point at which the force or moment exerted upon the bar is acting and the second to the point at which the displacement or rotation occurs |
| b | wall thickness |
| d | deflection at end of beam element; distance between spar uprights (web stiffeners) |
| E | Young's modulus |
| $f_b$ | bending stress in curved sheet of front spar |
| $f_B$ | maximum normal stress in element 3–5 at its midpoint |
| $f_c$ | normal stress in compression flange due to $f_{wt}$ |
| $f_{c_1}$ | normal stress in compression flange of front spar element due to bending resulting from T and $P_1$ |
| $f_{c_o}$ | normal stress in compression flange due to bending resulting from T |
| $f_s$ | shear stress in curved sheet of front spar element |
| $f_t$ | normal stress in tension flange due to $f_{wt}$ |
| $f_{t_1}$ | normal stress in tension flange of front spar element due to bending resulting from T and $P_1$ |
| $f_{t_o}$ | normal stress in tension flange due to bending resulting from T |
| $f_v$ | compressive stress in the uprights |
| $f_{wt}$ | tensile stress in the web parallel to the direction of wrinkles |
| G | shear modulus |
| h | distance between centroids of spar flanges |

| | |
|---|---|
| $\Sigma h_1$ | total length of uprights in a spar element |
| $I$ | moment of inertia |
| $I_1$ | moment of inertia of curved sheet and flanges of front spar |
| $I_F$ | moment of inertia of interspar element at front spar web |
| $I_x$ | moment of inertia of interspar element between spar webs at distance $x$ forward of rear spar |
| $I_{x'}$ | moment of inertia of interspar element between web and shear center of front spar, at distance $x'$ aft of shear center |
| $K$ | constant used in equations (9) |
| $L$ | length of beam element |
| $m$ | rotation at end of beam element |
| $\widehat{mm}$, $\widehat{mv}$ | influence coefficients |
| $M$ | end moment acting on beam element; bending moment at any section of front spar element due to $T$ and $P_1$ |
| $M_B$ | bending moment at the midpoint of element 3–5 |
| $M_3$ | moment acting on element 3–5 at joint 3 |
| $\widehat{nn}$ | influence coefficient |
| $n_1$, $n_2$, $n_3$, $n_4$, $n_5$, $n_6$ | rotations at ends of beam elements |
| $N_1$, $N_2$, $N_3$, $N_4$, $N_5$, $N_6$ | end moments |
| $P$ | total vertical load at end of front spar beam element |
| $P'$ | perimeter of the cross section of an interspar element between the web and shear center of front spar |
| $P_1$ | vertical load taken by curved sheet of front spar beam element |

| | |
|---|---|
| $P_3$ | vertical load on element 3–5 at joint 3 |
| $P_x$ | perimeter of the cross section of an interspar element between spar webs, at distance x forward of rear spar |
| Q | static moment of area used in shear-stress formula $f_s = PQ/It$ |
| $R.H.S._I$, $R.H.S._{II}$ | right-hand sides of equations of equilibrium, in which the subscripts refer to the condition of loading and end fixation |
| s | perimetric coordinate |
| t | web thickness |
| $t$, $t_1$, $t_2$, $t_3$, $t_4$, $t_5$, $t_6$ | rotations at ends of beam elements |
| $\widehat{tt}$, $\widehat{ty}$ | influence coefficients |
| $T$, $T_1$, $T_2$, $T_3$, $T_4$, $T_5$, $T_6$ | end moments |
| U, $U_{total}$ | total strain energy in a beam element |
| $U_{curved\ sheet}$ | strain energy in curved sheet of front spar element |
| $U_{flanges}$ | strain energy in flanges of front spar element |
| $U_{uprights}$ | strain energy in uprights of front spar element |
| $U_{web}$ | strain energy in flat web of front spar element |
| v | vertical displacement |
| $\widehat{vv}$, $\widehat{vm}$ | influence coefficients |
| V | shear force; volume |
| x, x' | horizontal coordinates |

| | |
|---|---|
| $y$ | vertical coordinate |
| $y$, $y_1$, $y_2$, $y_3$, $y_4$, $y_5$, $y_6$ | vertical displacements |
| $\widehat{yy}$, $\widehat{yt}$ | influence coefficients |
| $Y$, $Y_1$, $Y_2$, $Y_3$, $Y_4$, $Y_5$, $Y_6$ | shear forces |
| $\alpha$ | angle of folds of spar webs |
| $\theta$, $\phi$ | angular coordinates |
| $\omega$ | rotation |

## METHOD OF ANALYSIS

Figure 1 shows the wing structure that was analyzed and tested, and figures 2 and 3 are photographs of the wing on the test stand. For purposes of the analysis the actual structure was replaced by the assembly of bars shown in figure 4. The boxes consisting of two adjacent ribs, as well as the wing covering between them in the actual structure, are replaced in this figure by bars 1–2, 3–4, and 5–6. These bars are located at the chordwise center lines of the boxes and extend from the shear center of the D-shape front spar to the plane of the web of the rear spar. The spar elements extend spanwise from the center of one box to the center of the adjacent box and are located at the locus of the shear center of the front spar and at the web of the rear spar.

Each element is isolated and its ends are alternately assumed to be rigidly fixed. Calculations are then made of the forces and moments acting on the element at its free and fixed ends necessary to cause a unit vertical displacement without rotation or twist, a unit rotation in the plane of bending without vertical displacement or twist, and a unit twist without displacement or rotation in the plane of bending. These forces and moments at the ends of the elements are termed "influence coefficients."

Because of the principle of superposition, the sum of the products of the influence coefficients and the corresponding vertical and angular displacements must equal the external load on the structure at any one point. As many such equations may be written as there are unknown displacements. The matrix of the constant coefficients of the displacement

quantities in these equations in their final form is known as the "operations table." The solution of these simultaneous equations gives the displacements at the ends of the assumed elements for the given load condition. From these displacements and the influence coefficients the stresses at any point of the structure may be calculated.

In the calculation of the influence coefficients the spar elements were first assumed to have shear-resistant webs. Consequently, the moment of inertia of the rear spar section was computed considering the four flange angles and the entire section of the web as fully effective in bending. In the front spar the semicircular leading-edge skin was also included in the effective cross-sectional area. Solution of the resulting equations gave smaller deflections for the front spar than those observed in the experiments, while in the case of the rear spar the agreement was satisfactory. For this reason the calculations were repeated on the assumption that the shear webs acted as diagonal-tension fields, and the angle of the diagonals was taken as 30° since the folds observed in the test appeared to subtend approximately this angle. Calculations showed little effect of this angle on the displacements. This assumption resulted in good agreement between calculated and observed deflections in the case of the front spar, but in slightly exaggerated calculated deflections in the case of the rear spar. It might be mentioned here that the agreement between calculated and measured strains was generally better than that between calculated and observed deflections.

In the calculation of the influence coefficients of the interspar elements, namely, the boxes connecting the front spar with the rear spar, the variation in the height of the cross section was duly considered.

## CALCULATION OF THE INFLUENCE COEFFICIENTS

Upon the beam of figure 5 a shear force $V$ and an end moment $M$ are acting. It is known that the displacement $v$ and the rotation $m$ at the end can be calculated from the following formulas:

$$v = (1/3)VL^3/EI + (1/2)ML^2/EI \qquad (1)$$

$$m = (1/2)VL^2/EI + ML/EI \qquad (2)$$

As was stated earlier, in the Southwell and in the PIBAL methods

only one displacement quantity at a time is considered different from zero. For instance, it may be stipulated that the free end be displaced a unit distance in the vertical direction (downward) while the rotation is prevented by the constraints. Then with $v = 1$ and $m = 0$ equations (1) and (2) can be solved for $M$ and $V$:

$$M = -6EI/L^2 \tag{3}$$

$$V = 12EI/L^3 \tag{4}$$

These equations can be interpreted as expressing the values of the moment $M$ and the force $V$ exerted by the constraints upon the free end of the bar when this end is displaced downward and is prevented from rotating. By the definition given earlier, these are influence coefficients.

The influence coefficients corresponding to a unit rotation and zero vertical displacement can be obtained in a similar manner, if in equations (1) and (2) $v$ is set equal to zero and $m$ equal to unity. The solution is

$$M = 4EI/L \tag{5}$$

$$V = -6EI/L^2 \tag{6}$$

Influence coefficients are designated by two lower-case letters connected by an arc. The first letter refers to the force (or moment) exerted upon the bar, the second to the displacement (or rotation) that caused it; consequently, $\overset{\frown}{mv}$ is the moment caused by a unit vertical displacement, while $\overset{\frown}{vv}$ is the force caused by a unit vertical displacement. In order to indicate the points at which the force is acting and the displacement is taking place, two subscripts are used. The first subscript refers to the first lower-case letter in the symbol for the influence coefficient, and the second subscript to the second letter. With this convention equations (3) to (6) may be written in the form

$$\left.\begin{aligned} \widehat{mv}_{BB} &= -6EI/L^2 \\ \widehat{vv}_{BB} &= 12EI/L^3 \\ \widehat{mm}_{BB} &= 4EI/L \\ \widehat{vm}_{BB} &= -6EI/L^2 \end{aligned}\right\} \tag{7}$$

It may be noted that $\widehat{mv}_{BB} = \widehat{vm}_{BB}$, which equality is a consequence of Maxwell's reciprocal theorem.

The forces and moments exerted upon the fixed end of the beam of figure 5 as rigid end reactions can be calculated from the requirements of static equilibrium. They can be expressed with the aid of the influence-coefficient notation as follows:

$$\left.\begin{aligned} \widehat{mv}_{AB} &= \widehat{mv}_{BB} = -6EI/L^2 \\ \widehat{vv}_{AB} &= -\widehat{vv}_{BB} = -12EI/L^3 \\ \widehat{mm}_{AB} &= \widehat{mm}_{BA} = 2EI/L \\ \widehat{vm}_{AB} &= -\widehat{vm}_{BB} = 6EI/L^2 \end{aligned}\right\} \tag{8}$$

The sign convention used in these equations considers as positive downward forces and displacements as well as counterclockwise moments and rotations.

As is well known, equations (1) and (2) are valid only for beams

of constant moment of inertia. When the moment of inertia varies, as in the interspar members, the deflections and rotations must be obtained by integration. Numerical examples are given in appendix A. The torsional rigidity of the rear spar is small because of the nature of the construction. Advantage was taken of this fact in the calculation of the influence coefficients by assuming this torsional rigidity equal to zero. Accordingly, the rear spar cannot exert any end moments upon the interspar members, so that it becomes unnecessary to consider the effect of a prescribed rotation at the rear spar in a vertical plane containing the interspar member. When the vertical displacement of the interspar member is prescribed at its end at the rear spar, the member deflects as a cantilever with a concentrated load at its free end. When a vertical displacement or a rotation is stipulated at its front spar end, its rear spar end is considered as simply supported.

In appendix B influence coefficients of Wagner beams are developed using strain-energy methods. With the notation of figure 6 the results are:

$$\left.\begin{aligned} \widehat{ty}_{BB} &= \widehat{yt}_{BB} = E/[\,(L^2/Ah^2) - (K/L)\,] \\ \widehat{yy}_{BB} &= 2E/(K - L^3/Ah^2) \\ \widehat{tt}_{BB} &= (AEh^2/2)[(1/L) - L^2/(L^3 - h^2AK)] \end{aligned}\right\} \qquad (9a)$$

where

$$K = (8L/ht\,\sin^2 2\alpha) + (4L^3/3Ah^2) + (L\,\cot^2\alpha/A) + (2d^2\,\tan^2\alpha/h^2A_s)\sum h_1 \qquad (9b)$$

where A is the upper flange area, equal to that of the lower flange in this case. The influence coefficients at the fixed end can be calculated from the following equations:

$$\left.\begin{aligned} \widehat{ty}_{AB} &= \widehat{ty}_{BB} \\ \widehat{yy}_{AB} &= -\widehat{yy}_{BB} \\ \widehat{tt}_{AB} &= -(\widehat{tt}_{BB} + [\widehat{yt}_{BB}]L) \end{aligned}\right\} \tag{10}$$

The expressions for $\widehat{ty}_{BB}$, $\widehat{yy}_{BB}$, $\widehat{tt}_{BB}$, and $\widehat{yt}_{BB}$ are given in equations (9). The influence coefficients of a twisted thin-walled bar can be calculated from Bredt's formula

$$t = \frac{TL \oint (ds/b)}{4A_1^2 G} \tag{11}$$

where $t$ is the relative angle of twist between the two ends of the bar and $T$ is the torque. The integration must be carried out around the entire perimeter. Setting $t = 1$ and solving for $T$ yields

$$T = \widehat{tt} = \frac{4A_1^2 G}{L \oint (ds/b)} \tag{12}$$

It is easy to see that the influence coefficients for the fixed and free ends differ only in sign. When the cross section varies, the influence coefficients must be obtained by integration. For the interspar members this was done in appendix C. In view of the assumption that the torsional rigidity of the rear spar is zero, it is unnecessary to calculate influence coefficients corresponding to torsion of the rear spar.

The calculation of the influence coefficients of the D-shape front spar under shear force and bending moment leads to some complications when the flat web develops diagonal tension. Obviously, part of the shear force is transmitted by the diagonal-tension field and the rest by the curved leading-edge covering. The leading-edge covering did not develop wrinkles in the experiments. The normal stress is carried by the flanges and the curved sheet. The distribution of the shear force between the two elements was determined with the aid of Castigliano's second theorem. Of the total shear force $P$ the part taken by the flat web was $P - P_1$. The total strain energy stored in curved sheet,

flanges, web, and uprights, was calculated and its differential coefficient with respect to $P_1$ was set equal to zero. This yielded an expression for $P_1$ in terms of the load P, the end moment T, and the geometric and mechanical properties of the structure.

Substitution of $P_1$ in the expression for the total strain energy and differentiation with respect to P and T led to the end deflection and the end rotation, respectively, by virtue of Castigliano's first theorem. The influence coefficients could then be calculated as was done in the case of the beam with shear-resistant web. Details of the calculations are given in appendix D. Numerical values of the influence coefficients are collected in tables I to III.

## THE OPERATIONS TABLE

In the operations table are listed the forces and moments exerted upon each of the joints of the structure as a result of linear and angular displacements at the joints. The symbols used to denote forces, moments as well as linear and angular displacements, and the sign convention adopted, are shown in figure 7.

In order to explain how the entries in this table are calculated, let it be assumed that a positive unit rotation in the t-direction is undertaken at joint 3. (See fig. 8.) For convenience the unit chosen is $10^{-4}$ radian. The effect of this rotation upon all the joints of the structure must next be determined. However, as was stated earlier, whenever a displacement is undertaken, all the other possible displacements of the structure are assumed to be zero. In other words, the far ends of the members joined at 3 are considered to be rigidly fixed: The effect of a rotation at joint 3 is felt, therefore, only in members 1–3, 3–4, and 3–5.

It is apparent that the rotation stipulated will cause torsion in element 3–4. The moment that must be exerted upon this element to cause the prescribed rotation is the influence coefficient $\widehat{tt}$ shown in figure 8. In addition, moments $\widehat{tt}_{33}$ are needed to rotate elements 1–3 and 3–5 so that altogether a moment equal to $2\widehat{tt}_{33} + \widehat{tt}$ is required. If the properties of bars 1–3 and 3–5 were not the same, the moment $\widehat{tt}_{33}$ required to rotate each bar would be different. This is the case at joint 5, since the length of element 3–5 is 24 inches while that of element 5–7 is 12 inches. As may be seen from figure 8 the vertical forces that must act upon elements 1–3 and 3–5 at joint 3 are equal in magnitude and opposite in sense. They add up to a

zero resultant force. The forces and moments needed at the far ends of the elements are also indicated in figure 8. The numerical values of all these influence coefficients are listed in tables I and III.

The operations table corresponding to the assumption of shear-resistant spar webs is presented as table IV. Each of its columns contains the forces and moments at all the joints of the structure corresponding to the displacement indicated at the top of the column. The location and the nature of the force (whether a force, a moment in the n-direction, or a moment in the t-direction) are shown at the left end of each row. In the operations table are listed the reactions of the forces and moments which act upon the bars. Hence the entries in the operations table are the quantities calculated earlier multiplied by -1. In other words, the operations table contains the forces and moments exerted by the bars upon the assumed geometric constraints (the joints).

In the column headed $t_3$ the entries in the first five rows are zeros. This corresponds to the fact that a rotation in the t-direction at joint 3 has no effect upon joint 2 because of the assumption of rigid end fixation at the far ends of the bars. (See figs. 4 and 8.) Moreover, $t_3$ does not introduce a vertical force or a moment in the n-direction at joint 4. The next item is $T_4$, which is equal to 112.86580 inch-pounds when the webs are assumed to be shear resistant. The positive sign corresponds to the sign convention of figure 7 and to the fact that the operations table contains the forces and moments exerted upon the joints (or constraints). Eight digits are given, since little additional work is involved in keeping a large number of digits when a calculating machine is used and since it it desirable to have a great accuracy for checking purposes.

The next three rows refer to the effect of $t_3$ upon joint 6. Three zeros are listed since $t_3$ does not affect joint 6. At joint 3, $T_3$ is equal to $-(2\widehat{tt}_{33} + \widehat{tt})$, as was explained earlier. The numerical value is -407.42580 inch-pounds, which can be checked easily with the aid of tables I and III. Again, as in this entire discussion of table IV, the numerical values are those corresponding to shear-resistant webs. In row 11 a zero is entered because the vertical forces at joint 3 cancel, as was shown in the discussion of figure 8. In rows 12 to 15 are entered the influence coefficients for the fixed ends 1 and 5 multiplied by -1.

The entries in the other columns of the operations table are obtained in a similar manner. In addition to the operations table proper the so-called right-hand-side members are also listed in table IV. These represent the applied forces and moments acting on each of the joints.

In the calculations, as well as in the experiments, four conditions of end fixation and loading were considered. They are:

Condition I.- Both spars are rigidly fixed to the test rig at their ends (joints 7 and 8 in fig. 4) and a 500-pound load is acting downward on the rear spar 5 inches outboard of joint 1. Thus, for this condition the external vertical load on joint 1 is 500 pounds and the external moment in the t-direction is 2500 inch-pounds. The loads at all the other joints are zero. The operations table corresponding to these end conditions is presented in table IV, and the external loads are shown in the column headed $-R.H.S._I$.

Condition II.- The end fixation is the same as in condition I. A 500-pound load is acting downward on the rear spar at joint 3. Hence the external load at 3 is 500 pounds, while the external moment at 3, as well as the external loads at all the other joints, is zero. The operations table is contained in table IV and the external loads are listed in the column headed $-R.H.S._{II}$.

Condition III.- The front spar is rigidly fixed at joint 8 as before, but the attachment of the rear spar to the test rig at joint 7 is removed. The operations table is, of course, modified because of this change in the end conditions, but only the operations involving a vertical displacement $y_5$ and a rotation $t_5$ at joint 5 are affected. The quantities listed in table IV in the rows designated $T_5$ and $Y_5$ as well as in the columns headed $t_5$ and $y_5$ must be replaced by the following entries:

| | $t_5$ | $y_5$ |
|---|---|---|
| $T_5$ | -260.145798 | -9.20500 |
| $Y_5$ | -9.20500 | -3.0818933 |

The loading terms are the same as in condition I.

Condition IV.- The end fixation is the same as in condition III and the loading is the same as in condition II.

Table IV represents 2 sets of equations each containing 15 linear equations with 15 unknowns corresponding to conditions I and II. For example, row 1 can be read as follows:

$$-1325.907732n_2 - 54.560072y_2 + 39.926835n_4 + 54.560072y_1 = 0 \quad (13)$$

Row 13 represents the following equation if condition I (corresponding to $R.H.S._I$) is considered:

$$54.560072n_2 + 2.314819y_2 + 9.20500t_3 + 0.7670833y_3$$

$$+ 9.20500t_1 - 3.0818933y_1 = -500 \quad (14)$$

The operations table based on the assumption of fully developed tension diagonal field action is presented as table V. It was constructed in exactly the same manner as table IV, taking, however, from tables I and III the influence coefficients corresponding to Wagner beams.

The systems of linear equations were solved by matrix methods. Of these, Crout's procedure appears to be most advantageous (reference 9). The displacement quantities obtained by solving the systems of linear equations are listed in tables VI and VII for both assumptions of spar-web action.

## CALCULATION OF THE STRESSES

When the displacements and rotations are known at each joint, the forces and moments exerted upon the bars at the joints can be calculated easily with the aid of the influence coefficients. The shear force, the bending moment, and the torque at any point along the element can then be determined without difficulty from the laws of statics.

As an example, the normal stress will be computed in the flange at the midpoint of element 3-5 for condition I on the assumption of shear-resistant webs. The displacement quantities needed are taken from table VI:

$$y_3 = 0.39023 \text{ inch}$$

$$y_5 = 0.054731 \text{ inch}$$

$$t_3 = 0.015918 \text{ radian}$$

$$t_5 = 0.0078959 \text{ radian}$$

The influence coefficients of element 3–5 are rewritten from table I:

$$\widehat{yy}_{33} = 7670.8 \text{ pounds per inch}$$

$$\widehat{yt}_{33} = -92{,}050 \text{ pounds per radian}$$

$$\widehat{tt}_{33} = 1{,}472{,}800 \text{ inch-pounds per radian}$$

$$\widehat{yy}_{35} = -7670.8 \text{ pounds per inch}$$

$$\widehat{yt}_{35} = -92{,}050 \text{ pounds per radian}$$

$$\widehat{tt}_{35} = 736{,}400 \text{ inch pounds per radian}$$

The shear force on element 3–5 at joint 3 is:

$$P_3 = y_3(\widehat{yy}_{33}) + t_3(\widehat{yt}_{33}) + y_5(\widehat{yy}_{35}) + t_5(\widehat{yt}_{35}) \qquad (15)$$

The moment acting upon the element at joint 3 is:

$$M_3 = t_3(\widehat{tt}_{33}) + y_3(\widehat{ty}_{33}) + t_5(\widehat{tt}_{35}) + y_5(\widehat{ty}_{35}) \qquad (16)$$

Substitution of the numerical values yields:

$$P_3 = 381 \text{ pounds}$$

$$M_3 = -1624 \text{ inch-pounds}$$

Consequently, the bending moment $M_B$ at the midpoint of element 3–5 is:

$$M_B = 381 \times 12 - 1624 = 2954 \text{ inch-pounds}$$

Since the moment of inertia of the rear spar is 0.8416 inch$^4$ when the web is considered fully effective, the maximum stress $f_B$ in the flange is:

$$f_B = 2(2954)/(0.4208) = 7020 \text{ psi}$$

## DESCRIPTION OF THE EXPERIMENTS

In order to verify the theory, the aluminum-alloy model of a wing shown in figure 1 was designed, constructed, and tested. The wing comprised two spars, each having a thin-sheet web and four angle-section flanges formed on a bending brake. The curved leading-edge covering was attached to the flanges of the front spar so as to form a D-shape construction. The webs were stiffened by means of uprights riveted to them. Every third upright was part of a wing rib and was attached to the spar flanges as well as to the web. Tension diagonals developed in the web under comparatively low loads, probably because the stiffening effect of the shorter uprights was slight.

The curved portions of the flanges of the ribs were manufactured on a hydraulic press and were obtained through the courtesy of Edo Aircraft Corporation. The rib webs as well as the upper and lower cover plates of the wing were also stiffened by light angle sections which, however, seemed to be sufficiently rigid to prevent buckling. At least no waves, diagonals, or wrinkles could be observed in the webs of the ribs and in the cover plates during the experiments.

Three of the spaces between adjacent ribs were covered with skin, while the other three were left open to simulate cutouts. To the ends of the spars heavy machined steel fittings were riveted in order to provide attachments to the test rig strong enough to represent rigid end

fixation. Of the two end attachments the one at the front spar was always bolted to the test rig, while the one at the rear spar was bolted in test conditions I and II, and free in conditions III and IV.

Details of the construction and test arrangement may be seen in the photographs in figures 2 and 3. In order to provide for a suitable application of the concentrated loads, steel channels were riveted to both sides of the spar at locations corresponding to joint 3 and to a point 5 inches outboard of joint 1. (See fig. 4.) The external loads were applied to the steel channels by placing weights into a frame suspended from fittings attached to them.

Strains were measured by means of Baldwin Southwark SR-4 type A-1 metalectric strain gages cemented in pairs to the aft flanges (upper and lower) of the front spar and the forward flanges of the rear spar. Gages were located at the cutout sections of the wing at points A, B, C, D, E, and F in figure 4. The pairs of gages were connected in series in order to obtain the average value of the normal strain in each flange. An SR-4 control box was used for measuring the strain, and a brass plug and tapered socket arrangement was employed for switching. The accuracy of the strain measurements was checked by tests made with a cantilever beam to which pairs of gages were cemented. The maximum error in strain was found to be about $\pm 10 \times 10^{-6}$.

The absolute values of the strains measured in upper and lower flanges at the same location were found to be very much the same. As an example, the strains observed in the rear spar in loading condition I are shown in figure 9. Figure 10 demonstrates that the variation with load of the average absolute value of the strain at any location was linear. Similarly, the deflections increased proportionally to the loads, as may be seen in figure 11.

The deflections were measured at points 1, 2, 3, 4, 5, and 6 (fig. 4) by means of Ames dial gages placed on a sturdy steel frame rigidly attached to the test rig.

## COMPARISON OF THE RESULTS OF EXPERIMENT AND THEORY

The final results of the experiments are presented in figures 12 to 19, which contain the experimental curves of deflection and strain for the four conditions of loading. The values obtained by calculation are also shown in the same figures reduced to correspond to a load of 150 pounds in order to facilitate comparison with the experimental results. From such a comparison the following conclusions can be drawn:

Calculated strains agree well with the experimental values for both spars in all the four conditions of loading when diagonal-tension action is assumed in the spar webs. The only case in which there is appreciable disagreement is the strain in the rear spar for condition IV. However, in this case the strains are very small (at the point of greatest deviation $13 \times 10^{-6}$ corresponding to about 136-psi stress) and consequently hard to measure and unimportant for engineering purposes. When the webs are assumed to be shear resistant, the agreement is less satisfactory for the front spar and not much different from that obtained by the diagonal-tension assumption in the case of the rear spar.

As far as deflections are concerned, the diagonal-tension assumption gives good agreement for the front spar but not quite so good agreement for the rear spar for all conditions of loading. The shear-resistant-web assumption is better for the rear spar and less satisfactory for the front spar.

## CONCLUSIONS

The calculation of the strains in and the deflections of the spars of stressed-skin-type wings having cutouts can be carried out with a reasonable amount of work if the PIBAL method is used. Most of this work may be done by little-trained personnel. Time may be saved if use is made of the formulas developed in this report for the influence coefficients. Experiments with a model wing gave satisfactory agreement with the theory for four different conditions of loading and end fixation.

Polytechnic Institute of Brooklyn,
Brooklyn, N. Y., August 23, 1946.

## APPENDIX A

## DEFLECTIONS AND ROTATIONS OF BEAM ELEMENT WITH VARIABLE MOMENT OF INERTIA

In calculating the vertical displacement at the aft end of the interspar element for a unit load at this end, the variable moment of inertia of the element (rib flanges, rib web, wing covering) between the rear spar and the front spar webs was calculated to be

$$I_x = 0.000016x^3 + 0.00624x^2 + 0.2400x + 2.4416 \qquad (A1)$$

where $x$ is measured from the rear spar. In the analysis based upon the assumption of shear-resistant spar webs, the moment of inertia was assumed to vary hyperbolically between the front spar web and the shear center of the D-section, being infinite at the latter point, and may be written as

$$I_{x'} = 3.57I_F/x'$$

where $x'$ is measured from the shear center; 3.57 inches is the distance between the shear center and the front spar web, and $I_F$ is the moment of inertia of the interspar element at the front spar web.

By making use of the unit-load method, the total displacement at the aft end for unit load at this end is expressed by

$$d = 1/E \int_0^{20} x^2\, dx/I_x + (1/3.57I_FE) \int_0^{3.57} x'(23.57 - x')^2\, dx' \qquad (A2)$$

The first integration was performed numerically by Simpson's rule, which is explained in reference 10. The numerical value of the vertical displacement is

$$d = 43.20 \times 10^{-6} \text{ in./unit load}$$

To calculate the rotation at the forward end due to a unit moment in a vertical plane containing the interspar element, the unit-load method is again employed. For the assumptions of shear-resistant spar webs and zero torsional rigidity of the rear spar,

$$\omega = 1/E \int_{3.57}^{23.57} (1 - x'/23.57)^2 \, dx'/I_x + (1/3.57 I_F E) \int_{0}^{3.57} x'(1 - x'/23.57) \, dx' \qquad (A3)$$

where $\omega$ is the angle of rotation at the front spar in radians. The numerical value is

$$\omega = 0.07776 \times 10^{-6} \text{ radian /unit moment}$$

It may be mentioned here that in the analysis for the assumption of Wagner beam action the interspar elements were assumed to have infinite rigidity between the front spar web and the shear center of the front spar.

Because of the assumption of no torsional rigidity for the rear spar, for a typical interspar element 3-4 the influence coefficients $\widehat{nn}_{33}$, $\widehat{ny}_{33}$, $\widehat{yn}_{33}$, $\widehat{ny}_{34}$, $\widehat{yn}_{43}$, $\widehat{nn}_{34}$, $\widehat{nn}_{43}$ are zero. The remaining influence coefficients may be obtained from the values of $d$ and $\omega$ with the aid of formulas (A4).

$$\left.\begin{aligned} \widehat{yy}_{33} = -\widehat{yy}_{43} = \widehat{yy}_{44} = -\widehat{yy}_{34} = 1/d \\ \widehat{nn}_{44} = 1/\omega \\ \widehat{yn}_{44} = \widehat{ny}_{44} = 1/(23.57\omega) \\ \widehat{yn}_{34} = \widehat{ny}_{43} = -23.57/d \end{aligned}\right\} \qquad (A4)$$

## APPENDIX B

## WAGNER BEAM INFLUENCE COEFFICIENTS

The total strain energy in the Wagner beam spar element shown in figure 6 may be expressed as

$$U = (1/2E)\left[f_{wt}^2\, htL + \int_0^L (f_t + f_{t_o})^2 A_t\, dx + \int_0^L (f_c + f_{c_o})^2 A_c\, dx + f_v^2 A_s \Sigma h_1\right] \tag{B1}$$

where $t$ is the web thickness. It may be stated that

$$\left.\begin{aligned} f_{wt} &= 2Y/(ht \sin 2\alpha) \\ f_t &= (Y/A_t)[(x/h) - (1/2)\cot\alpha] \\ f_c &= -(Y/A_c)[(x/h) + (1/2)\cot\alpha] \\ f_v &= Yd \tan\alpha/(hA_s) \\ f_{t_o} &= T/(A_t h) \\ f_{c_o} &= -T/(A_c h) \end{aligned}\right\} \tag{B2}$$

The expressions for $f_{wt}$, $f_t$, $f_c$, and $f_v$ are derived in the theory of tension field webs developed by H. Wagner and summarized by

Paul Kuhn in reference 11. In the expression for $f_v$, d is the distance between uprights.

On substituting these expressions in equation (B1) and integrating, the total strain energy becomes

$$U = \frac{1}{2E}\left[\frac{4Y^2L}{ht\sin^2 2\alpha} + \frac{2L^3Y^2}{3Ah^2} + \frac{LY^2\cot^2\alpha}{2A} + \frac{2YTL^2}{Ah^2} + \frac{2T^2L}{Ah^2} + \frac{Y^2d^2\tan^2\alpha\,\Sigma h_1}{A_s h^2}\right] \tag{B3}$$

In this equation $A = A_c = A_t$.

By virtue of Castigliano's first theorem the partial derivative of U with respect to Y yields the total vertical displacement d due to Y and T, and the partial derivative of U with respect to T yields the total rotation t due to Y and T, d and E being measured at the free end of the element.

$$\left.\begin{aligned}\frac{\partial U}{\partial Y} = d = (1/2E)\left[\frac{8YL}{ht(\sin 2\alpha)^2} + \frac{4L^3Y}{3Ah^2} + \frac{LY\cot^2\alpha}{A} + \frac{2L^2T}{Ah^2} + \frac{2Yd^2\tan^2\alpha\,\Sigma h_1}{A_s h^2}\right]\\ \frac{\partial U}{\partial T} = t = \frac{YL^2 + 2LT}{AEh^2}\end{aligned}\right\} \tag{B4}$$

Then with $d = 1$ and $t = 0$, as in the case of equations (1) and (2), equations (B4) are solved for T and Y. In the notation of the influence coefficients $T = \widehat{tv}_{BB}$ and $Y = \widehat{vv}_{BB}$.

In order to obtain the influence coefficients corresponding to a unit rotation and zero vertical displacement, equations (B4) are solved $d = 0$ and $t = 1$. In the notation of the influence coefficients $T = \widehat{tt}_{BB}$ and $Y = \widehat{yt}_{BB} = \widehat{ty}_{BB}$. The values of the influence coefficients are given in equations (9).

## APPENDIX C

## INFLUENCE COEFFICIENT FOR TORSION OF BEAM ELEMENT WITH VARIABLE MOMENT OF INERTIA

For the interspar members in this analysis, the wall thickness of a cross section is constant, $\oint ds$ is replaced by $P_x$ and $A$ by $A_x$; $P_x$ and $A_x$ are the perimeter and area of a cross section, respectively, at a distance $x$ forward of the rear spar, for $x$ less than 20 inches. In the notation of figure 20,

$$\left.\begin{aligned} P_x &= 4(0.1x + 8) \\ A_x &= 48(1 + 0.05x) \end{aligned}\right\} \qquad (C1)$$

For $x$ greater than 20 inches, again in the notation of figure 20, the perimeter and area of a cross section of the member are given by

$$\left.\begin{aligned} P' &= 2(2y + 12) \\ A' &= 24y \end{aligned}\right\} \qquad (C2)$$

Consequently, equation (12) becomes

$$\widehat{tt} = 4Gb \int_0^L \frac{A_x^2}{P_x}\,dx + 4Gb \int_0^d \frac{A'^2}{P'}\,dx \qquad (C3)$$

The numerical value obtained is

$$\widehat{tt} = 1.128658 \times 10^6 \text{ in.-lb/radian}$$

## APPENDIX D

## FRONT-SPAR INFLUENCE COEFFICIENTS

Figure 21 shows a sketch of the curved sheet and the flanges of the D-shape front spar, which carry the part $P_1$ of the total vertical load P, and the end moment T. If $f_s$ represents the shear stress and $f_b$ the bending stress, the strain energy stored in the curved sheet is

$$U_{\text{curved sheet}} = \int_V \frac{f_s^2}{2G}\,dV + \int_V \frac{f^2}{2E}\,dV \qquad (D1)$$

the integration being performed over the entire volume. Or, in the notation of figure 21,

$$U_{\text{curved sheet}} = \frac{1}{2G}\int_0^{\pi}\left(\frac{P_1 Q}{I_1 t}\right)^2 rtL\,d\varphi$$

$$+ \frac{1}{2E}\int_0^{L}\int_0^{\pi}\left(\frac{Mr\cos\varphi}{I_1}\right)^2 tr\,d\varphi\,dx$$

where

$$Q = \frac{Ah}{2} + \int_0^{\varphi} r^2 t \cos\theta \, d\theta = \frac{Ah}{2} + r^2 t \sin\varphi \qquad (D2)$$

$$I_1 = \frac{\pi r^3 t}{2} + 2A\left(\frac{h}{2}\right)^2$$

$$M = T + P_1 x$$

It will be noted that the flanges carry an additional normal stress due to Wagner beam action. To calculate the strain energy stored in the Wagner beam a procedure similar to that given in appendix B is used. The strain energy in the web is

$$U_{web} = \frac{1}{2E} \int_V f_{wt}^2 \, dV = \frac{2(P - P_1)^2 L}{Eht(\sin 2\alpha)^2} \qquad (D3)$$

The total strain energy stored in the flanges is

$$U_{flanges} = \frac{1}{2E}\left[\int_0^L \left(f_t + f_{t_1}\right)^2 A \, dx + \int_0^L \left(f_c + f_{c_1}\right)^2 A \, dx\right] \qquad (D4)$$

where $f_t$ is the normal stress in the tension flange due to Wagner beam action, $f_{t_1}$ the normal stress in the tension flange due to bending resulting from $(T + P_1 x)$ of figure 21, and $f_c$ and $f_{c_1}$ have corresponding meanings for the compression flange. From the discussion in appendix B it follows that

$$\left.\begin{aligned} f_t &= \frac{P - P_1}{A}\left(\frac{x}{h} - \frac{\cot\alpha}{2}\right) \\ f_c &= -\frac{P - P_1}{A}\left(\frac{x}{h} + \frac{\cot\alpha}{2}\right) \\ f_{t_1} &= \frac{(T + P_1 x)h}{2I_1} \\ f_{c_1} &= \frac{(T + P_1 x)h}{2I_1} \end{aligned}\right\} \tag{D5}$$

Substituting these values in equation (D4) and integrating yields

$$U_{flanges} = \frac{A}{2E}\left[\frac{2(P - P_1)^2 L^3}{3A^2h^2} + \frac{(P - P_1)^2 L \cot^2\alpha}{2A^2} + \frac{2(P - P_1)L^2}{AI_1}\left(\frac{T}{2} + \frac{PL}{3}\right) + \frac{h^2 L}{2I_1^2}\left(T^2 + TP_1L + \frac{P_1^2L^2}{3}\right)\right] \tag{D6}$$

The strain energy stored in the uprights of the Wagner beam is

$$U_{uprights} = \frac{(P - P_1)^2 d^2 \Sigma h_1 \tan^2\alpha}{2Eh^2A_s} \tag{D7}$$

The total vertical displacement $d$ and rotation $t$ at the free end resulting from $T$ and $P$ are found from

$$\left.\begin{aligned} d &= \frac{\partial U_{total}}{\partial P} = \frac{\partial U_{curved\ sheet}}{\partial P} + \frac{\partial U_{web}}{\partial P} + \frac{\partial U_{flanges}}{\partial P} + \frac{\partial U_{uprights}}{\partial P} \\ t &= \frac{\partial U_{total}}{\partial T} = \frac{\partial U_{curved\ sheet}}{\partial T} + \frac{\partial U_{web}}{\partial T} + \frac{\partial U_{flanges}}{\partial T} + \frac{\partial U_{uprights}}{\partial T} \end{aligned}\right\} \quad (D8)$$

However, it will be noted that the expression for $U_{total}$ contains $P_1$, the undetermined part of the total vertical load taken by the curved sheet. By Castigliano's second theorem

$$\frac{\partial U_{total}}{\partial P_1} = 0 \quad (D9)$$

When $P_1$ is determined from equation (D9) and the result substituted in the expression for $U_{total}$, equations (D8) yield d and t. Then proceeding as in appendix B and substituting the numerical constants for the element under consideration yield

$$\widehat{yy}_{BB} = 13,767.55 \text{ lb/in.}$$

$$\widehat{ty}_{BB} = -165,210.65 \text{ in.-lb/in.}$$

$$\widehat{tt}_{BB} = 4,378,361.09 \text{ in.-lb/radian}$$

$$\widehat{yt}_{BB} = \widehat{ty}_{BB}$$

$$\widehat{tt}_{AB} = -(24\widehat{yt}_{BB} + \widehat{tt}_{BB})$$

$$= -413,305.439 \text{ in.-lb/radian}$$

The numerical constants used to obtain these results are:

$L = 24$ in.

$h = 7.6$ in

$\Sigma h_1 = 35\frac{3}{4}$ in.

$t = 0.020$ in.

$d = 4$ in.

$\alpha = 30^\circ$

$A_s = 0.06$ sq in.

$A = 0.12$ sq in.

$r = 4$ in.

$I_1 = 5.4762$ in.$^4$

$E = 10.5 \times 10^6$ psi

$G = 3.9 \times 10^6$ psi

## REFERENCES

1. Ballenstedt, L.: Influence of Ribs on Strength of Spars. NACA TN No. 139, 1923.

2. Friedrichs, K., and Kármán, Th.: Zur Berechnung freitragender Flügel. Aerodynamischen Institut an der Technischen Hochschule Aachen, No. 9, 1930.

3. von Fákla, Stefan: Bending and Torsion Stiffness of Cantilever Wings. Luftfahrtforschung, vol. 4, no. 1, June 5, 1929, pp. 30-40 (Air Corps trans. No. 262).

4. Williams, D., and Cox, H. Roxbee: The Effect of the Ribs on the Stresses in the Spars of a Two Spar Wing Subjected to the Most General Type of Loading. R. & M. No. 1538, 1933, pp. 525-537.

5. Kuhn, Paul: Analysis of 2-Spar Cantilever Wings with Special Reference to Torsion and Load Transference. NACA Rep. No. 508, 1935.

6. Goodey, W. J.: Two Spar Wing Stress Analysis. Aircraft Engineering, London, vol. 13, June 1941, pp. 150-153.

7. Hoff, N. J., Levy, Robert S., and Kempner, Joseph: Numerical Procedures for the Calculation of the Stresses in Monocoques. I - Diffusion of Tensile Stringer Loads in Reinforced Panels. NACA TN No. 934, 1944.

   Hoff, N. J., and Kempner, Joseph: Numerical Procedures for the Calculation of the Stresses in Monocoques. II - Diffusion of Tensile Stringer Loads in Reinforced Flat Panels with Cut-Outs. NACA TN No. 950, 1944.

   Hoff, N. J., Libby, Paul A., and Klein, Bertram: Numerical Procedures for the Calculation of the Stresses in Monocoques. III - Calculation of the Bending Moments in Fuselage Frames. NACA TN No. 998, 1946.

   Hoff, N. J., Klein, Bertram, and Libby, Paul A.: Numerical Procedures for the Calculation of the Stresses in Monocoques. IV - Influence Coefficients of Curved Bars for Distortions in Their Own Plane. NACA TN No. 999, 1946.

   Hoff, N. J., Boley, Bruno A., and Klein, Bertram: Stresses in and General Instability of Monocoque Cylinders with Cutouts. II - Calculation of the Stresses in a Cylinder with a Symmetric Cutout. NACA TN No. 1014, 1946.

8. Southwell, R. V.: Relaxation Methods in Engineering Science, a Treatise on Approximate Computation. Clarendon Press (Oxford), 1940.

9. Crout, Prescott D.: A Short Method for Evaluating Determinants and Solving Systems of Linear Equations with Real or Complex Coefficients. Trans. A.I.E.E., vol. 60, 1941, p. 1235.

10. von Kármán, Theodore, and Biot, Maurice: Mathematical Methods in Engineering. McGraw-Hill Book Co., Inc., 1940, pp. 3-6.

11. Kuhn, Paul: A Summary of Design Formulas for Beams Having Thin Webs in Diagonal Tension. NACA TN No. 469, 1933.

TABLE I.- REAR-SPAR INFLUENCE COEFFICIENTS

| Influence coefficients | Shear-resistant web | Wagner beam |
|---|---|---|
| Element 1-3[a] | | |
| $Y_1\widehat{y}_1$, $Y_3\widehat{y}_3$ | 7,670.833 | 2,172.291 |
| $T_1\widehat{y}_1$, $Y_1\widehat{t}_1$, $T_3\widehat{y}_1$, $Y_1\widehat{t}_3$ | -92,050.000 | -26,067.488 |
| $T_1\widehat{t}_1$, $T_3\widehat{t}_3$ | 1,472,800 | 653,009.833 |
| $T_1\widehat{t}_3$, $T_3\widehat{t}_1$ | 736,400.000 | -27,390.169 |
| $T_3\widehat{y}_3$, $Y_3\widehat{t}_3$, $Y_3\widehat{t}_1$, $T_1\widehat{y}_3$ | 92,050.000 | 26,067.488 |
| $Y_3\widehat{y}_1$, $Y_1\widehat{y}_3$ | -7,670.833 | -2,172.291 |
| Element 5-7 | | |
| $Y_5\widehat{y}_5$ | 61,366.66 | 6,135.8718 |
| $T_5\widehat{y}_5$, $Y_5\widehat{t}_5$, $T_7\widehat{y}_5$ | -368,200.000 | -36,815.231 |
| $T_5\widehat{t}_5$ | 2,945,600 | 901,291.383 |
| $Y_7\widehat{y}_5$ | -61,366.66 | -6,135.8718 |
| $T_7\widehat{t}_5$ | 1,472,800 | -459,508.615 |
| $Y_7\widehat{t}_5$ | 368,200 | -36,815.231 |

[a]For element 3-5 the influence coefficients are identical with the corresponding ones given for element 1-3.

TABLE II.- FRONT-SPAR INFLUENCE COEFFICIENTS

| Influence coefficients | Shear-resistant web | Wagner beam |
|---|---|---|
| Element 2-4[a] | | |
| $Y_2\widehat{y_2}$, $Y_4\widehat{y_2}$ | 62,066.211 | 13,767.5543 |
| $T_2\widehat{y_2}$, $Y_2\widehat{t_2}$, $T_4\widehat{y_2}$, $Y_2\widehat{t_4}$ | -744,794.531 | 165,210.6517 |
| $T_2\widehat{t_2}$, $T_4\widehat{t_4}$ | 11,916,712.50 | 4,378,361.087 |
| $T_2\widehat{t_4}$, $T_4\widehat{t_2}$ | 5,958,356.25 | -413,305.439 |
| $T_4\widehat{y_4}$, $Y_4\widehat{t_4}$, $Y_4\widehat{t_2}$, $T_2\widehat{t_4}$ | 744,794.531 | 165,210.651 |
| $Y_4\widehat{y_2}$, $Y_2\widehat{y_4}$ | -62,066.211 | -13,767.5543 |
| Element 6-8 | | |
| $Y_6\widehat{y_6}$ | 496,529.69 | 41,561.5189 |
| $T_6\widehat{y_6}$, $Y_6\widehat{t_6}$, $T_6\widehat{y_6}$ | -2,979,178.12 | -249,369.114 |
| $T_6\widehat{t_6}$ | 23,833,425 | 6,287,872.293 |
| $T_6\widehat{t_6}$ | 11,916,712.5 | -3,295,442.925 |
| $Y_6\widehat{y_6}$ | -496,529.69 | -41,561.5189 |
| $Y_8\widehat{t_6}$ | 2,979,178.12 | 249,369.114 |

[a]For element 4-6 the influence coefficients are identical with the corresponding ones given for element 2-4.

TABLE III.- INFLUENCE COEFFICIENTS FOR THE INTERSPAR ELEMENTS

| Influence coefficients[1] | Shear-resistant-web assumption | Wagner-beam assumption | Unit |
|---|---|---|---|
| $\widehat{yy}_{rr} = \widehat{yy}_{ff}$ | 23,148.10 | 34,319.578 | lb/in. |
| $\widehat{tt}_{ff} = -\widehat{tt}_{rf} = \widehat{tt}_{rr} = -\widehat{tt}_{fr}$ | 1,128,658.0 | 1,260,652.5 | in.-lb/in. |
| $\widehat{nn}_{ff} = \widehat{nn}_{rr}$ | 12,859,809 | 17,613,632.5 | in.lb/radian |
| $\widehat{yn}_{rf} = -\widehat{yn}_{ff}$ | 545,600.72 | 732,132.04 | lb/radian |

[1]Subscript f refers to front spar; subscript r refers to rear spar.

NATIONAL ADVISORY
COMMITTEE FOR AERONAUTICS

| | | $n_2$ | $y_2$ | $t_2$ | $n_4$ | $y_4$ | $t_4$ | $n_6$ | $y_6$ | $t_6$ | $t_3$ | $y_3$ | $t_1$ | $y_1$ | $t_5$ | $y_5$ | $-RHS_1$ | $-RHS_2$ |
|---|---|---|---|---|---|---|---|---|---|---|---|---|---|---|---|---|---|---|
| 1 | $N_2$ | −1328.807732 | −54.560072 | 0 | 39.926835 | 0 | 0 | 0 | 0 | 0 | 0 | 0 | 0 | 54.560072 | 0 | 0 | 0 | 0 |
| 2 | $Y_2$ | −54.560072 | −8.521431 | 74.479453 | 0 | 6.2068211 | 74.479453 | 0 | 0 | 0 | 0 | 0 | 0 | 2.31481 | 0 | 0 | 0 | 0 |
| 3 | $T_2$ | 0 | 74.479453 | −1304.83705 | 0 | −74.479453 | −595.835825 | 0 | 0 | 0 | 0 | 0 | 112.885798 | 0 | 0 | 0 | 0 | 0 |
| 4 | $N_4$ | 39.926835 | 0 | 0 | −1385.834857 | −54.560072 | 0 | 39.926835 | 0 | 0 | 0 | 54.560072 | 0 | 0 | 0 | 0 | 0 | 0 |
| 5 | $Y_4$ | 0 | 6.2068211 | −74.479453 | −54.560072 | −14.72805 | 0 | 0 | 6.298621 | 74.479453 | 0 | 2.31481 | 0 | 0 | 0 | 0 | 0 | 0 |
| 6 | $T_4$ | 0 | 74.479453 | −595.835825 | 0 | 0 | −2496.208 | 0 | −74.479453 | −595.835825 | 112.88568 | 0 | 0 | 0 | 0 | 0 | 0 | 0 |
| 7 | $N_6$ | 0 | 0 | 0 | 39.926835 | 0 | 0 | −1405.761482 | −54.560072 | 0 | 0 | 0 | 0 | 0 | 0 | 54.560072 | 0 | 0 |
| 8 | $Y_6$ | 0 | 0 | 0 | 0 | 6.2068211 | −74.479453 | −54.560072 | −58.174400 | 223.438359 | 0 | 0 | 0 | 0 | 0 | 2.31481 | 0 | 0 |
| 9 | $T_6$ | 0 | 0 | 0 | 0 | 74.479453 | −595.835825 | 0 | 223.438359 | −3887.87985 | 0 | 0 | 0 | 0 | 112.885798 | 0 | 0 | 0 |
| 10 | $T_3$ | 0 | 0 | 0 | 0 | 0 | 112.88580 | 0 | 0 | 0 | −107.42580 | 0 | −73.84000 | 9.20800 | −73.84000 | −9.20580 | 0 | 0 |
| 11 | $Y_3$ | 0 | 0 | 0 | 54.560072 | 2.31481 | 0 | 0 | 0 | 0 | 0 | −2.64898 | −8.20580 | 0.7678833 | 9.20600 | 0.7678833 | 0 | 500 |
| 12 | $T_1$ | 0 | 0 | 112.885798 | 0 | 0 | 0 | 0 | 0 | 0 | −73.84000 | −8.20580 | −280.145798 | 9.20800 | 0 | 0 | 2500 | 0 |
| 13 | $Y_1$ | 54.560072 | 2.31481 | 0 | 0 | 0 | 0 | 0 | 0 | 0 | 9.20600 | 0.7678833 | 9.205800 | −2.0818833 | 0 | 0 | 500 | 0 |
| 14 | $T_5$ | 0 | 0 | 0 | 0 | 0 | 0 | 0 | 0 | 112.885798 | −73.84000 | 9.205800 | 0 | 0 | −854.785798 | 27.615000 | 0 | 0 |
| 15 | $Y_5$ | 0 | 0 | 0 | 0 | 0 | 0 | 54.560072 | 2.31481 | 0 | −9.20580 | 0.7678833 | 0 | 0 | 27.615800 | −9.2185399 | 0 | 0 |

TABLE IV.- OPERATIONS TABLE FOR THE ASSUMPTION OF SHEAR-RESISTANT SPAR WEBS.

NATIONAL ADVISORY
COMMITTEE FOR AERONAUTICS

| | | $n_2$ | $v_2$ | $l_2$ | $n_4$ | $v_4$ | $l_4$ | $n_6$ | $v_6$ | $l_6$ | $l_5$ | $v_5$ | $l_1$ | $v_1$ | $l_6$ | $v_6$ | $-RHS_1$ | $-RHS_2$ |
|---|---|---|---|---|---|---|---|---|---|---|---|---|---|---|---|---|---|---|
| 1 | $N_2$ | −1601.2961385 | −73.2132038 | 0 | 39.9268837 | 0 | 0 | 0 | 0 | 0 | 0 | 0 | 0 | 73.2132038 | 0 | 0 | 0 | 0 |
| 2 | $Y_2$ | −73.2132036 | −4.41998181 | 16.52106517 | 0 | 1.37875643 | 16.52106517 | 0 | 0 | 0 | 0 | 0 | 0 | 3.04319578 | 0 | 0 | 0 | 0 |
| 3 | $T_2$ | 0 | 16.52106517 | −583.9013567 | 0 | −16.52106517 | 41.3305439 | 0 | 0 | 0 | 0 | 0 | 126.065248 | 0 | 0 | 0 | 0 | 0 |
| 4 | $N_4$ | 39.9268837 | 0 | 0 | −1841.2176222 | −73.2132038 | 0 | 39.9268837 | 0 | 0 | 0 | 73.2132038 | 0 | 0 | 0 | 0 | 0 | 0 |
| 5 | $Y_4$ | 0 | 1.37875643 | −16.52106517 | −73.2132038 | −5.79870884 | 0 | 0 | 1.37875643 | 16.52106517 | 0 | 3.04319578 | 0 | 0 | 0 | 0 | 0 | 0 |
| 6 | $T_4$ | 0 | 16.52106517 | 41.3305439 | 0 | 0 | −400.7374884 | 0 | −16.52106517 | 41.3305439 | 126.065248 | 0 | 0 | 0 | 0 | 0 | 0 | 0 |
| 7 | $N_6$ | 0 | 0 | 0 | 39.9268837 | 0 | 0 | −1861.1438098 | −73.2132038 | 0 | 0 | 0 | 0 | 0 | 0 | 73.2132038 | 0 | 0 |
| 8 | $Y_6$ | 0 | 0 | 0 | 0 | 1.37875643 | −16.52106517 | −73.2132038 | −8.57610310 | 8.41584623 | 0 | 0 | 0 | 0 | 0 | 3.04319578 | 0 | 0 |
| 9 | $T_6$ | 0 | 0 | 0 | 0 | 16.52106517 | 41.3305439 | 0 | 8.41584623 | −1192.686598 | 0 | 0 | 0 | 0 | 126.065248 | 0 | 0 | 0 |
| 10 | $T_3$ | 0 | 0 | 0 | 0 | 0 | 126.065248 | 0 | 0 | 0 | −254.6872145 | 0 | 2.73901685 | 2.6067486 | 2.73901685 | −2.6067486 | 0 | 0 |
| 11 | $Y_3$ | 0 | 0 | 0 | 73.2132038 | 3.04319578 | 0 | 0 | 0 | 0 | 0 | −2.47705386 | −2.6067486 | 0.21722905 | 2.6067486 | 0.21722905 | 0 | 500 |
| 12 | $T_1$ | 0 | 0 | 126.065248 | 0 | 0 | 0 | 0 | 0 | 0 | 2.73901685 | −2.6067486 | −191.36833125 | 2.6067486 | 0 | 0 | 2500 | 0 |
| 13 | $Y_1$ | 73.2132038 | 3.04319578 | 0 | 0 | 0 | 0 | 0 | 0 | 0 | 2.6067486 | 0.21722905 | 2.6067486 | −3.25043483 | 0 | 0 | 500 | 0 |
| 14 | $T_5$ | 0 | 0 | 0 | 0 | 0 | 0 | 0 | 0 | 126.065248 | 2.73901685 | 2.6067486 | 0 | 0 | −281.49538957 | 1.074774278 | 0 | 0 |
| 15 | $Y_5$ | 0 | 0 | 0 | 0 | 0 | 0 | 73.2132038 | 3.04319578 | 0 | −2.6067486 | 0.21722905 | 0 | 0 | 1.074774468 | −3.874012068 | 0 | 0 |

TABLE V.- OPERATIONS TABLE FOR THE ASSUMPTION OF WAGNER-BEAM SPAR ELEMENTS.

TABLE VI

SOLUTION OF MATRICES FOR THE ASSUMPTION OF SHEAR-RESISTANT WEBS

[Linear and Angular Displacements times $10^4$]

| Condition | I (500-lb load at end; both spars fixed) | II (500-lb load at joint 3; both spars fixed) | III (500-lb load at end; rear spar free) | IV (500-lb load at joint 3; rear spar free) |
|---|---|---|---|---|
| $n_2$ radians | 160.24 | 82.702 | 310.98 | 227.89 |
| $y_2$ inches | 4619.7 | 1720.1 | 5,232.9 | 2125.0 |
| $t_2$ radians | 124.65 | 39.849 | 136.52 | 47.401 |
| $n_4$ radians | 84.315 | 66.539 | 233.83 | 211.41 |
| $y_4$ inches | 1919.4 | 792.40 | 2,249.1 | 1016.2 |
| $t_4$ radians | 98.647 | 37.092 | 110.36 | 44.628 |
| $n_6$ radians | 14.342 | 13.141 | 147.57 | 147.58 |
| $y_6$ inches | 239.49 | 111.51 | 307.13 | 161.11 |
| $t_6$ radians | 39.751 | 18.435 | 49.509 | 25.174 |
| $t_3$ radians | 159.18 | 66.529 | 172.51 | 74.191 |
| $y_3$ inches | 3902.3 | 2388.0 | 7,767.3 | 6033.6 |
| $t_1$ radians | 179.62 | 44.217 | 191.69 | 51.752 |
| $y_1$ inches | 8452.1 | 3681.2 | 12,619 | 7508.5 |
| $t_5$ radians | 78.959 | 54.528 | 108.13 | 68.645 |
| $y_5$ inches | 547.31 | 401.39 | 3,938.3 | 3808.8 |

NATIONAL ADVISORY
COMMITTEE FOR AERONAUTICS

TABLE VII

SOLUTION OF MATRICES FOR WAGNER-BEAM ASSUMPTION

[Linear and Angular Displacements times $10^4$]

| Condition | I (500-lb load at end; both spars fixed) | II (500-lb load at joint; both spars fixed) | III (500-lb load at end; rear spar free) | IV (500-lb load at joint; rear spar free) |
|---|---|---|---|---|
| $n_2$ radians | 0.023305 | 0.013069 | 0.036220 | 0.025316 |
| $y_2$ inches | 59731 | .22769 | .67828 | .28398 |
| $t_2$ radians | .015446 | .0048967 | .016833 | .0059464 |
| $n_4$ radians | .013163 | .012013 | .025987 | .021016 |
| $y_4$ inches | .25218 | .11187 | .29998 | .14094 |
| $t_4$ radians | .012297 | .0046496 | .013664 | .0055411 |
| $n_6$ radians | .0033627 | .0032997 | .015063 | .015008 |
| $y_6$ inches | .032725 | .016946 | .048969 | .030393 |
| $t_6$ radians | .0050065 | .0023852 | .0061564 | .0030680 |
| $t_3$ radians | .00170180 | .0069400 | .018568 | .0078426 |
| $y_3$ inches | .56867 | .40506 | .92556 | .64747 |
| $t_1$ radians | .019828 | .0051996 | .021238 | .0060373 |
| $y_1$ inches | 1.1635 | .54267 | 1.5552 | .89538 |
| $t_5$ radians | .0081012 | .0052501 | .011183 | .0067089 |
| $y_5$ inches | .11195 | .095177 | .42183 | .40454 |

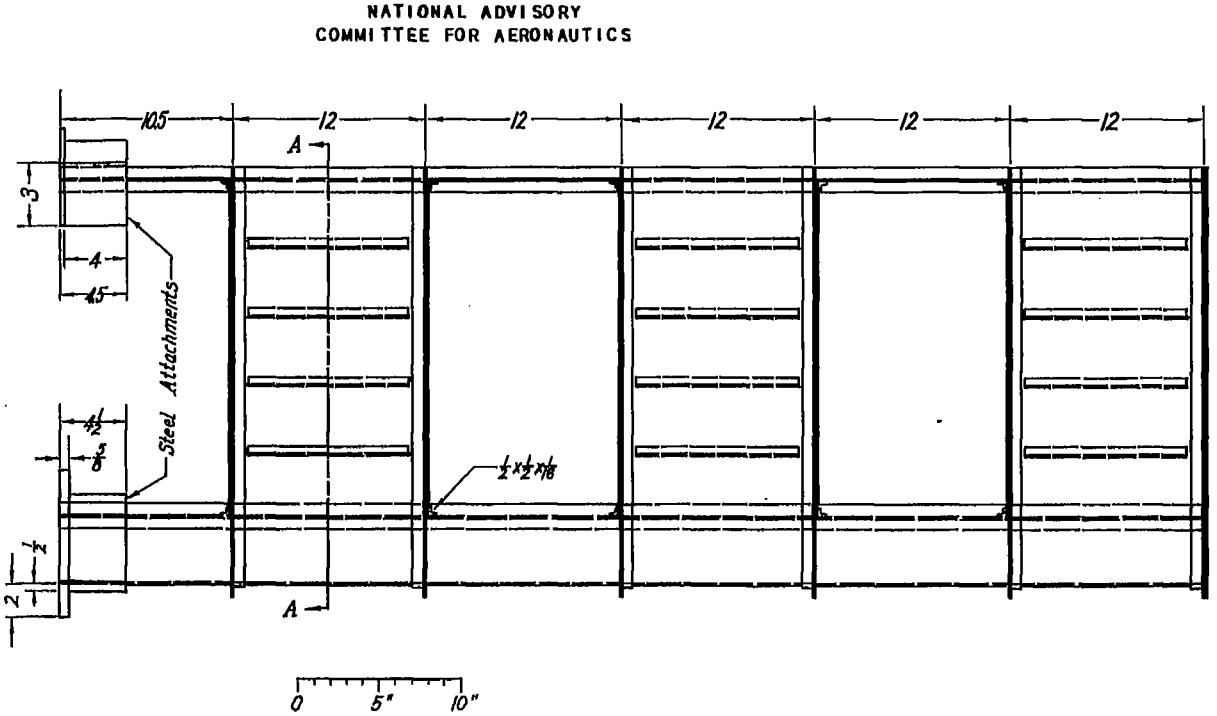


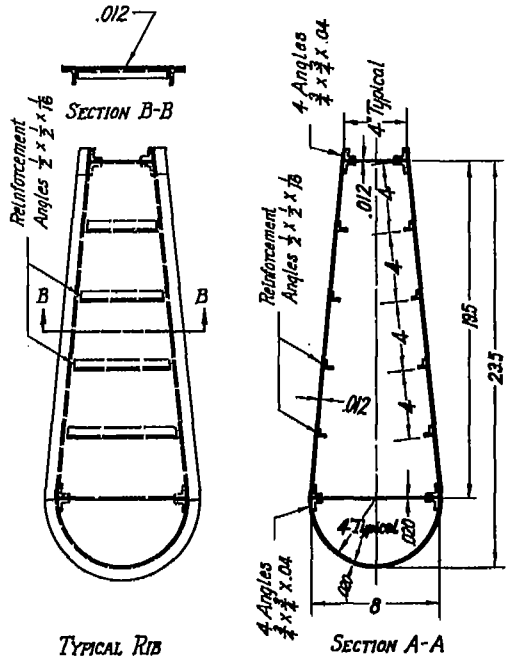


FIGURE 1.- TEST SPECIMEN.

MATERIAL: 24S-T ALUMINUM ALLOY

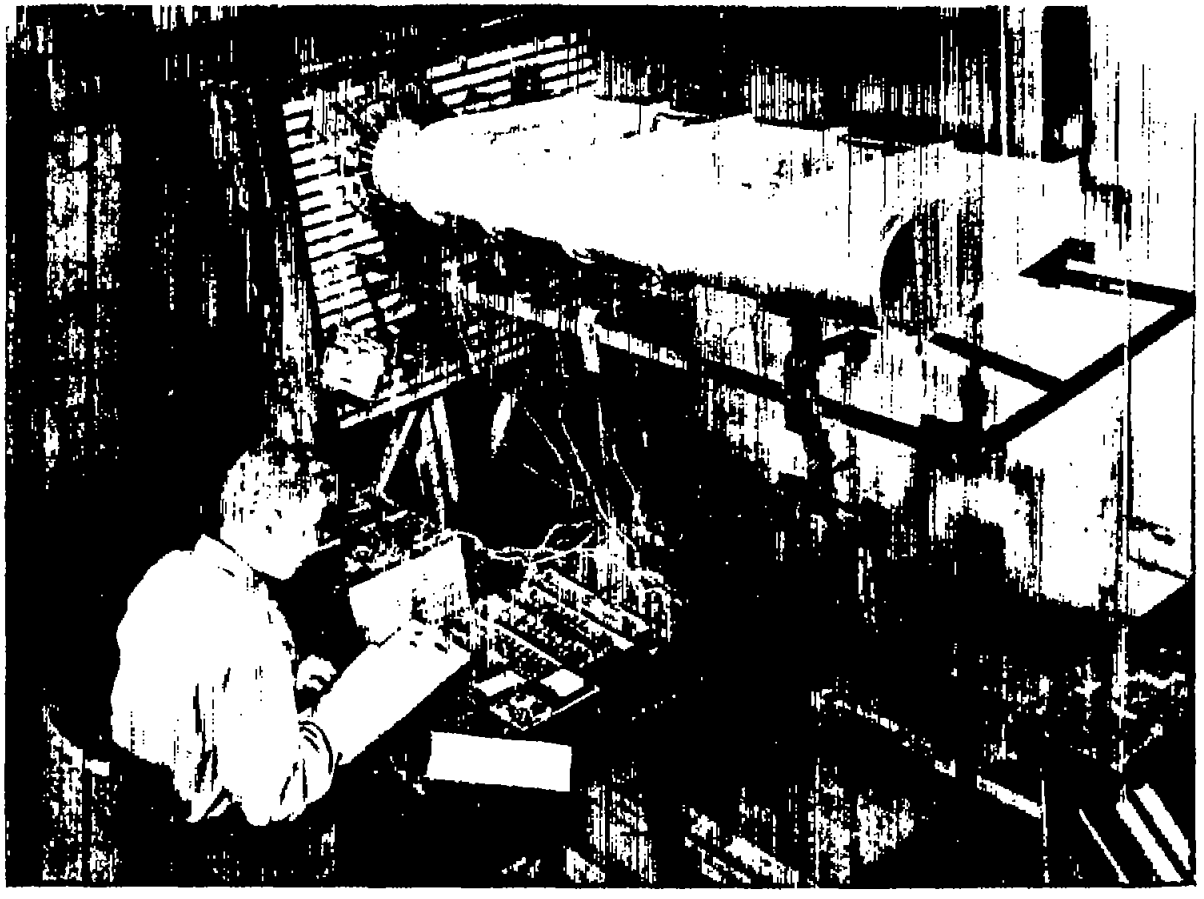

Figure 2.- Front view of wing model and test apparatus.

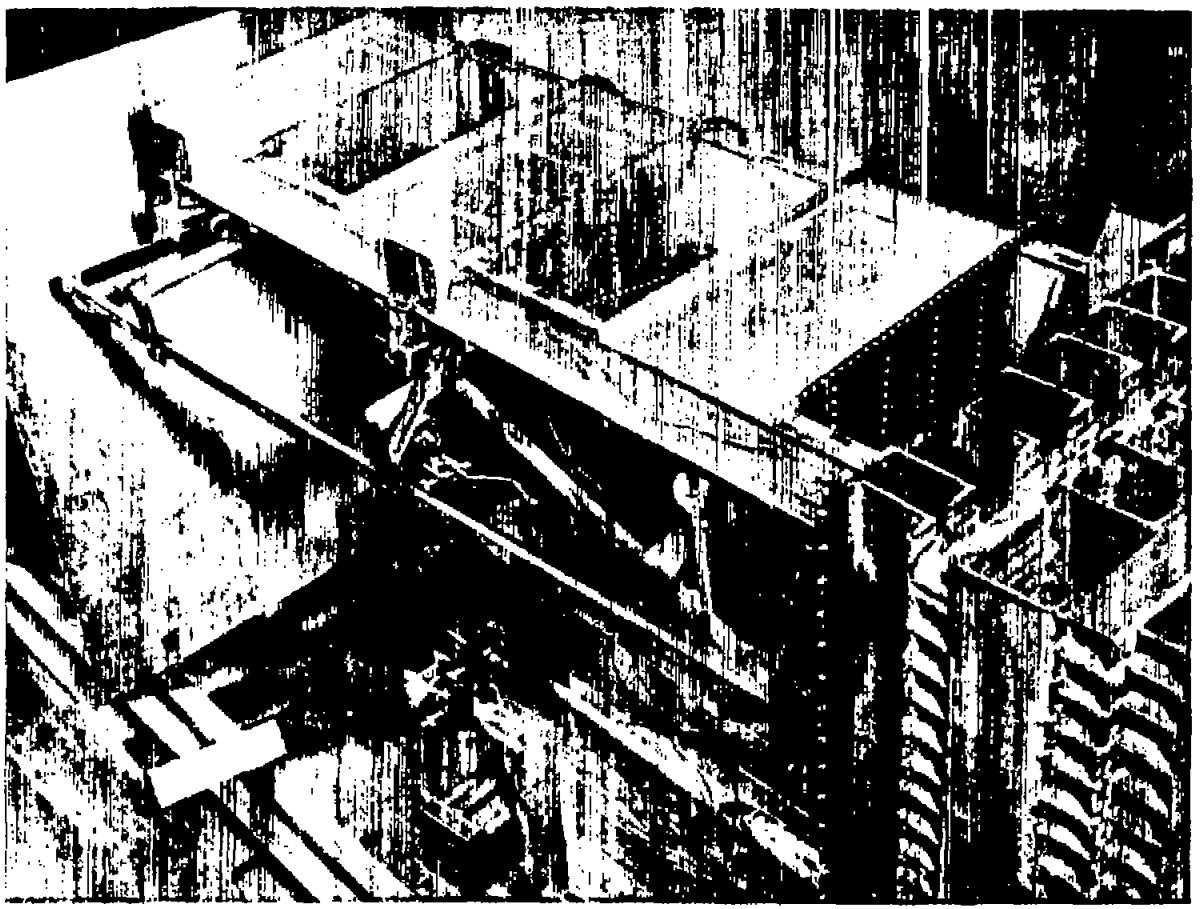

Figure 3.- Rear view of wing model and test apparatus.

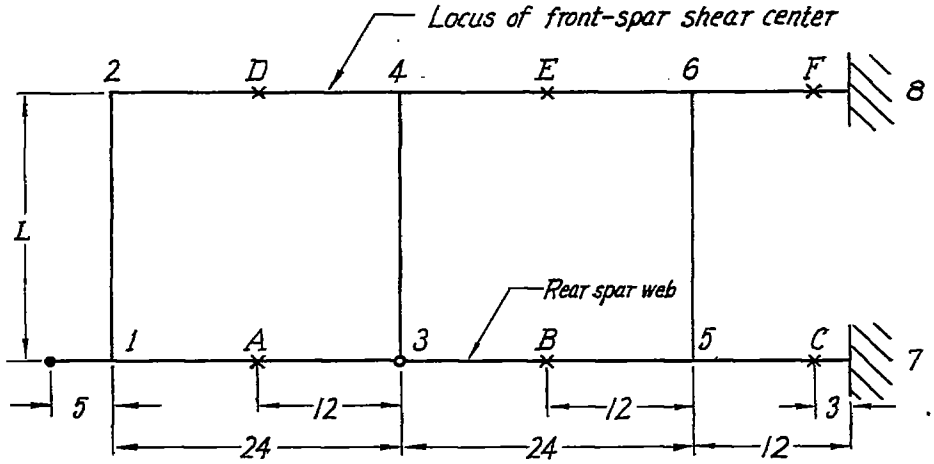


1,2,3,4,5,6, indicate location of Ames gages
Letters indicate location of strain gages

L = 23.57 in first matrix
L = 24.06 in second matrix

Point of load application
- ○ tests II and IV
- ● tests I and III

NATIONAL ADVISORY COMMITTEE FOR AERONAUTICS

Figure 4.- Simplified structure assumed in analysis.

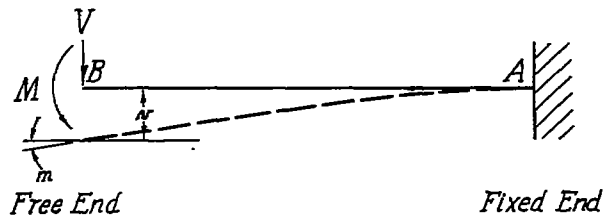


Note: Directions shown are positive

Figure 5.- Beam element for calculation of influence coefficients.

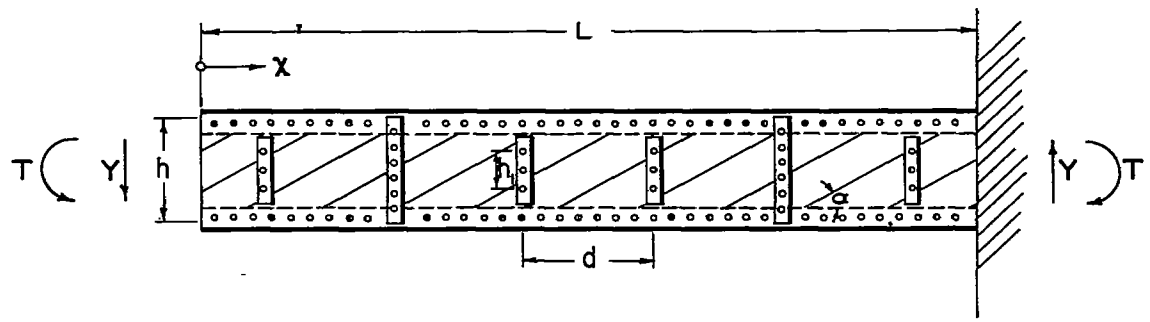


Figure 6.- Wagner beam element

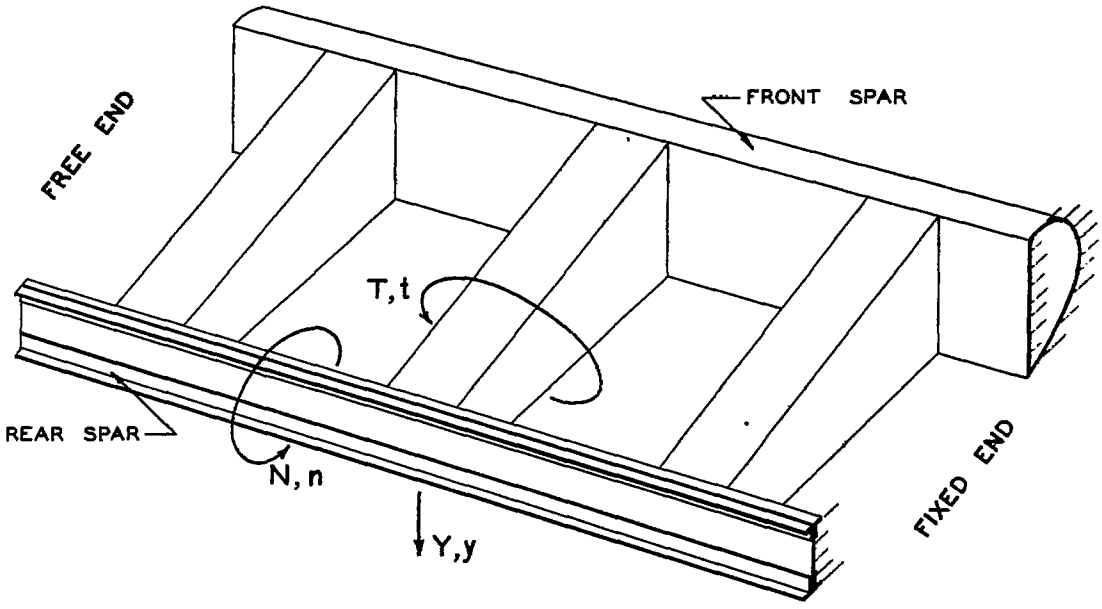


Figure 7.- Sign convention of forces, moments, linear and angular displacements.

(All directions shown are positive; upper-case letters represent forces and moments; lower-case letters represent vertical and angular displacements.)



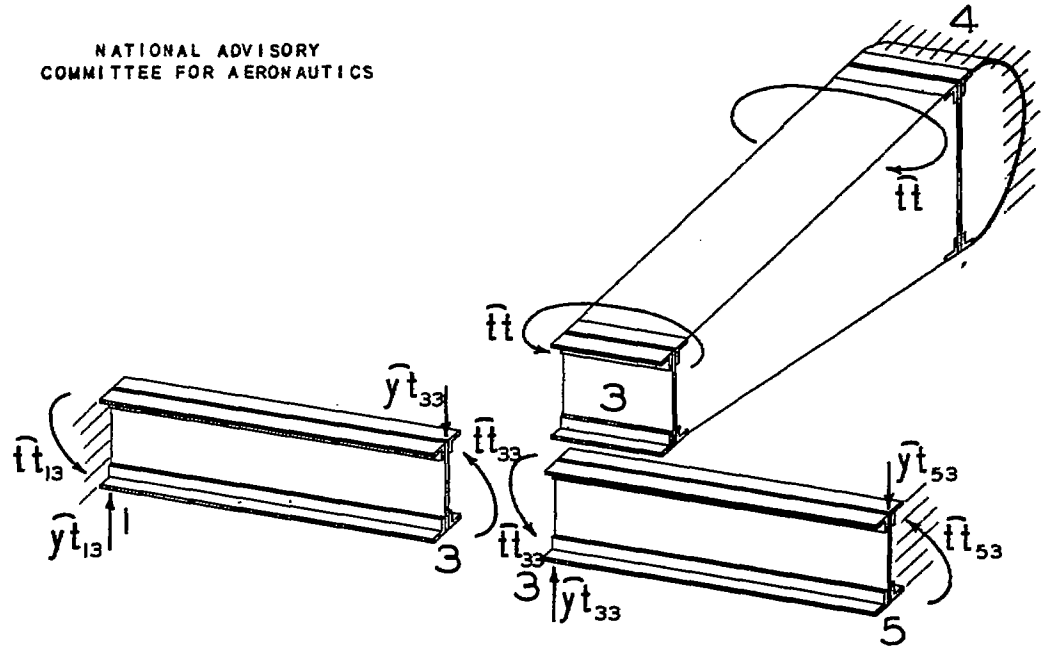


Figure 8.- Effect of a unit rotation at joint 3 in the t-direction.

(The influence coefficients shown represent the absolute values of the forces and moments exerted upon the structural elements by the constraints; the arrows indicate the directions in which they act.)

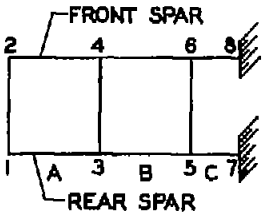


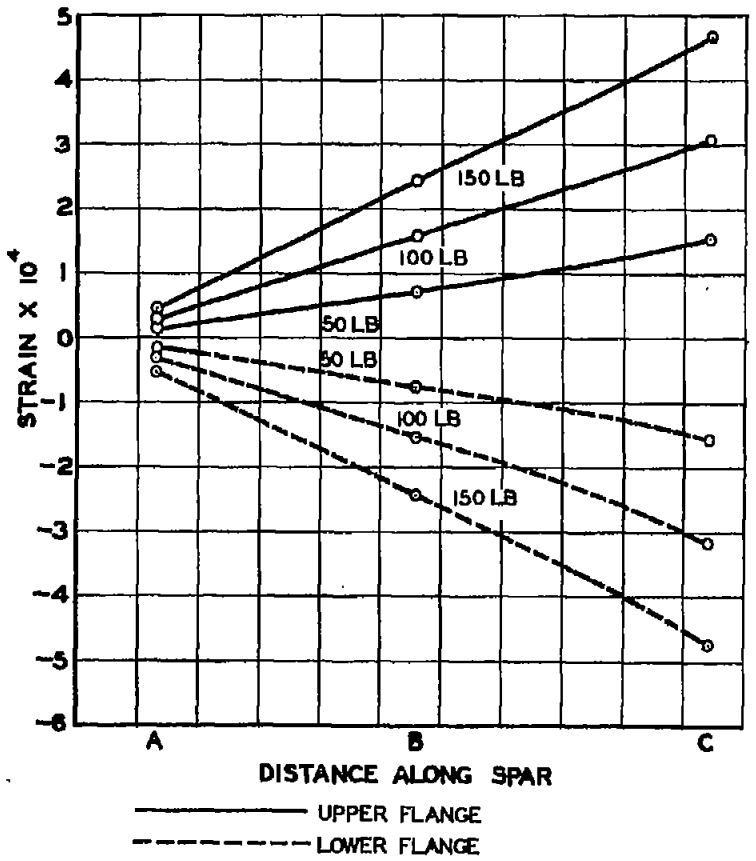


Figure 9.- Experimental strains in upper and lower flanges, rear spar. Condition I.

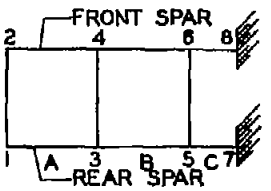


NATIONAL ADVISORY
COMMITTEE FOR AERONAUTICS

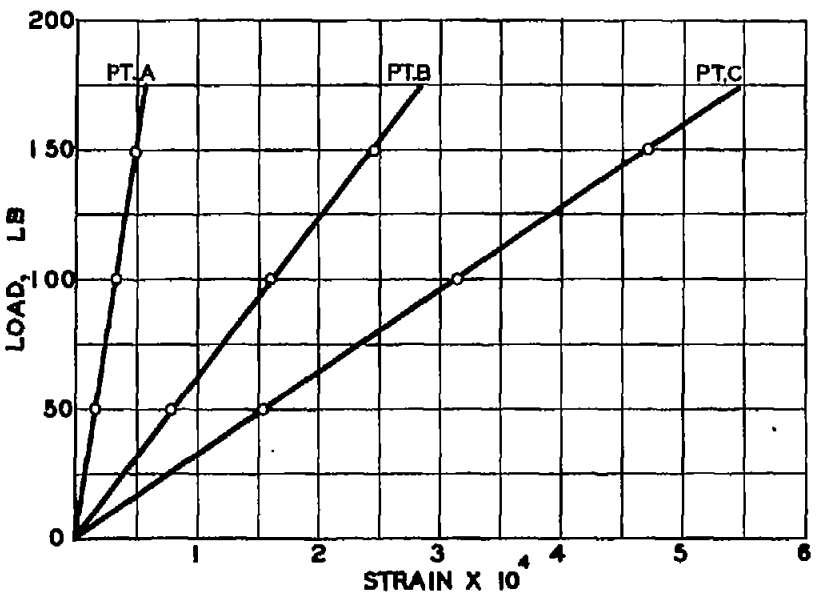


Figure 10.- Variation of strain with load, from experiment, rear spar. Condition I.

(Strains are averages of absolute values measured in upper and lower flanges.)

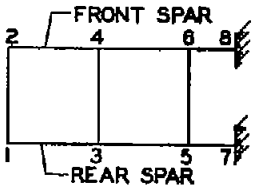


NATIONAL ADVISORY
COMMITTEE FOR AERONAUTICS

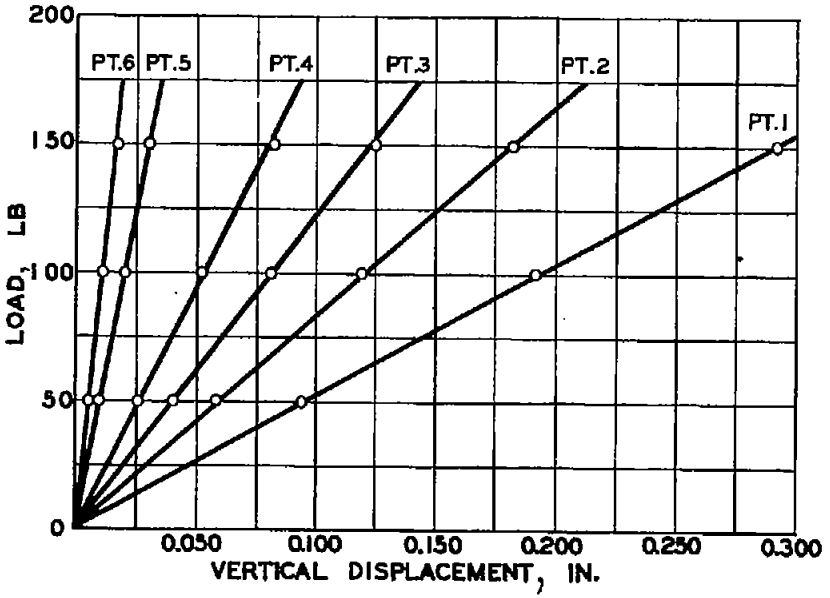


Figure 11.- Variation of deflections with load, from experiment, both spars. Condition I.

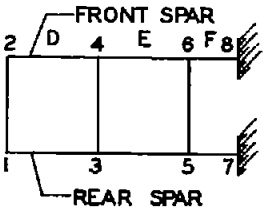


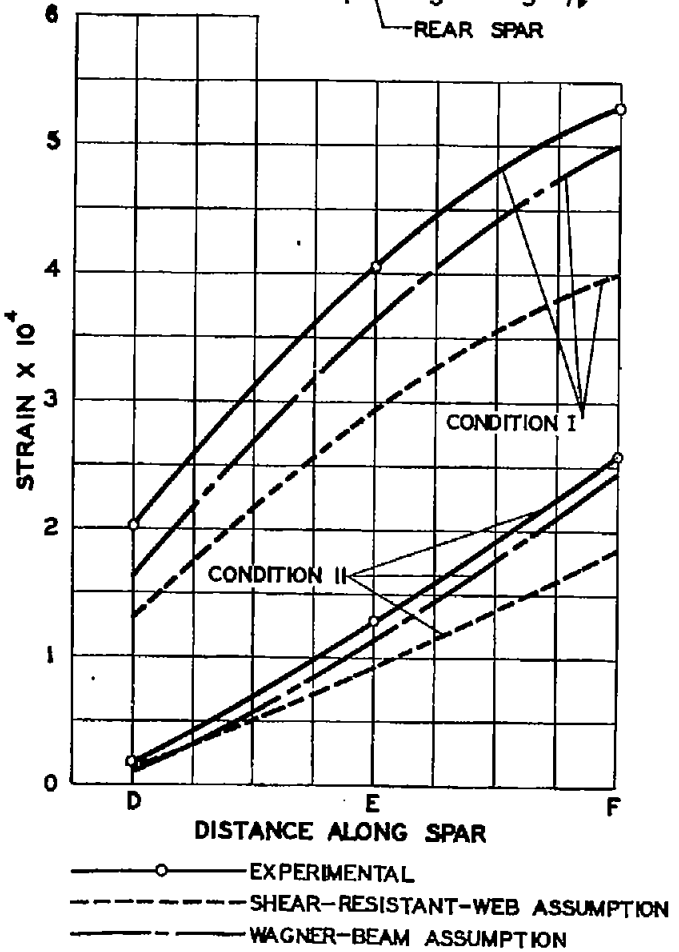


Figure 12.- Experimental and theoretical strains, front spar. Conditions I and II; load, 150 pounds.

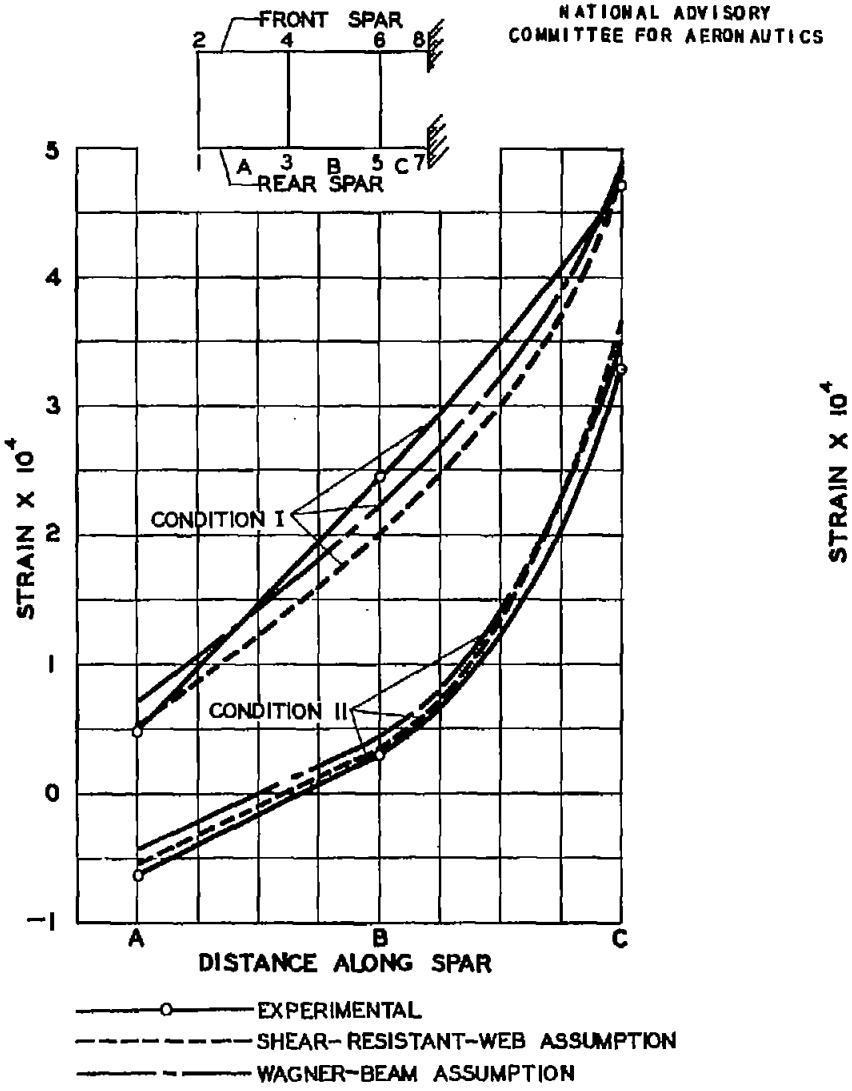


Figure 13.- Experimental and theoretical strains, rear spar. Conditions I and II; load, 150 pounds.

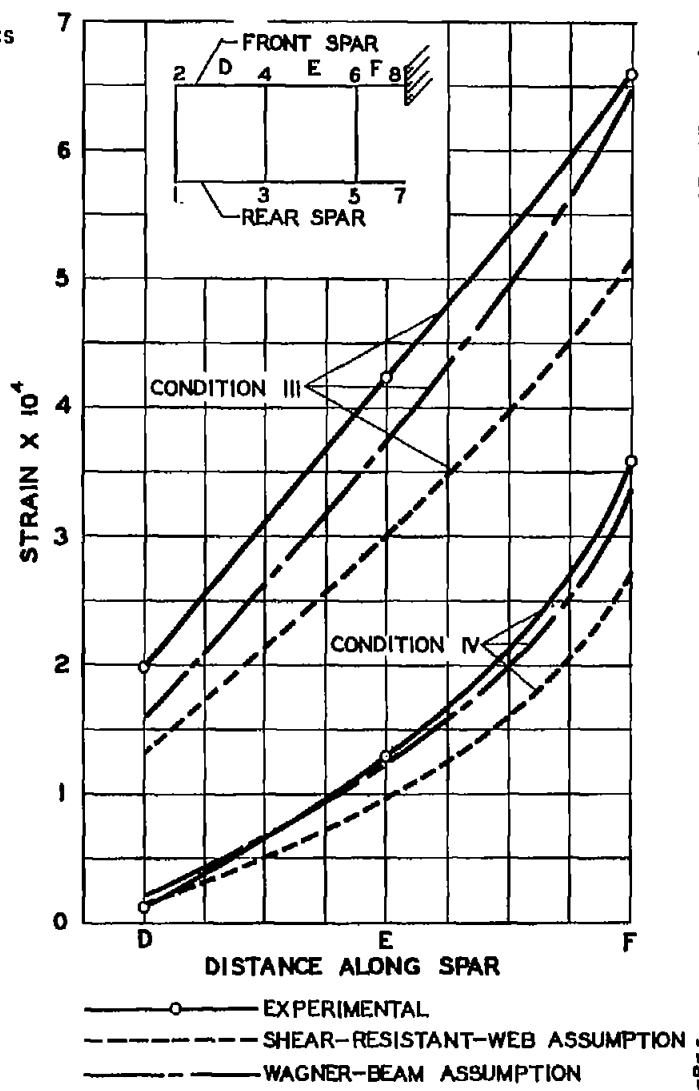


Figure 14.- Experimental and theoretical strains, front spar. Conditions III and IV; load, 150 pounds.

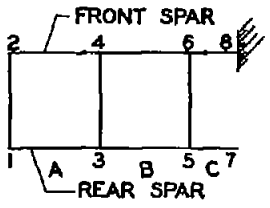


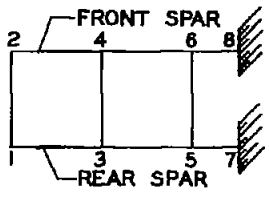


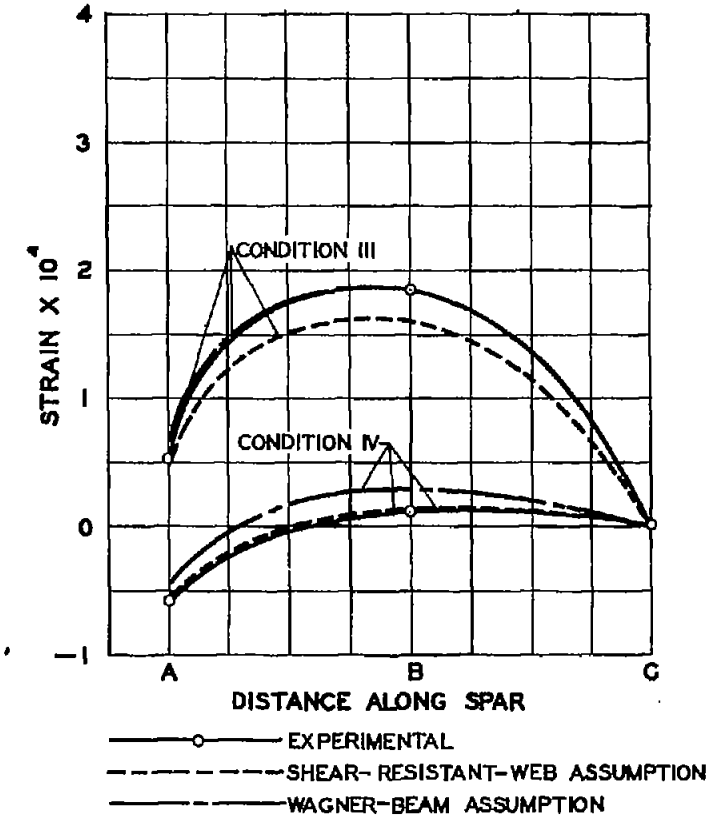


Figure 15.- Experimental and theoretical strains, rear spar. Conditions III and IV; load, 150 pounds.

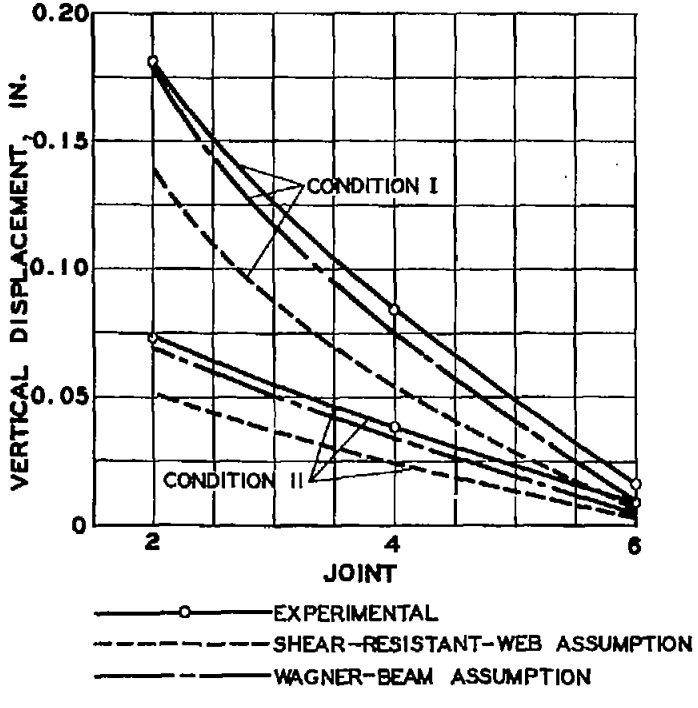


Figure 16.- Experimental and theoretical vertical displacements, front spar. Conditions I and II; load, 150 pounds.

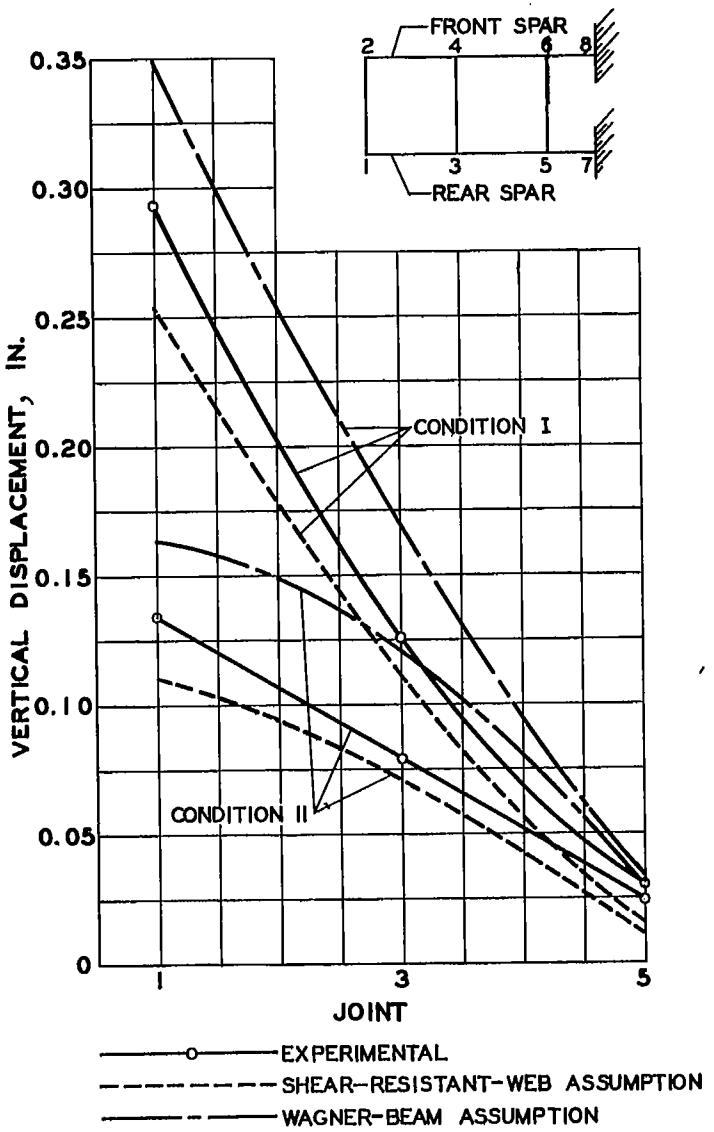


Figure 17.- Experimental and theoretical vertical displacements, rear spar. Conditions I and II; load, 150 pounds.

NATIONAL ADVISORY
COMMITTEE FOR AERONAUTICS

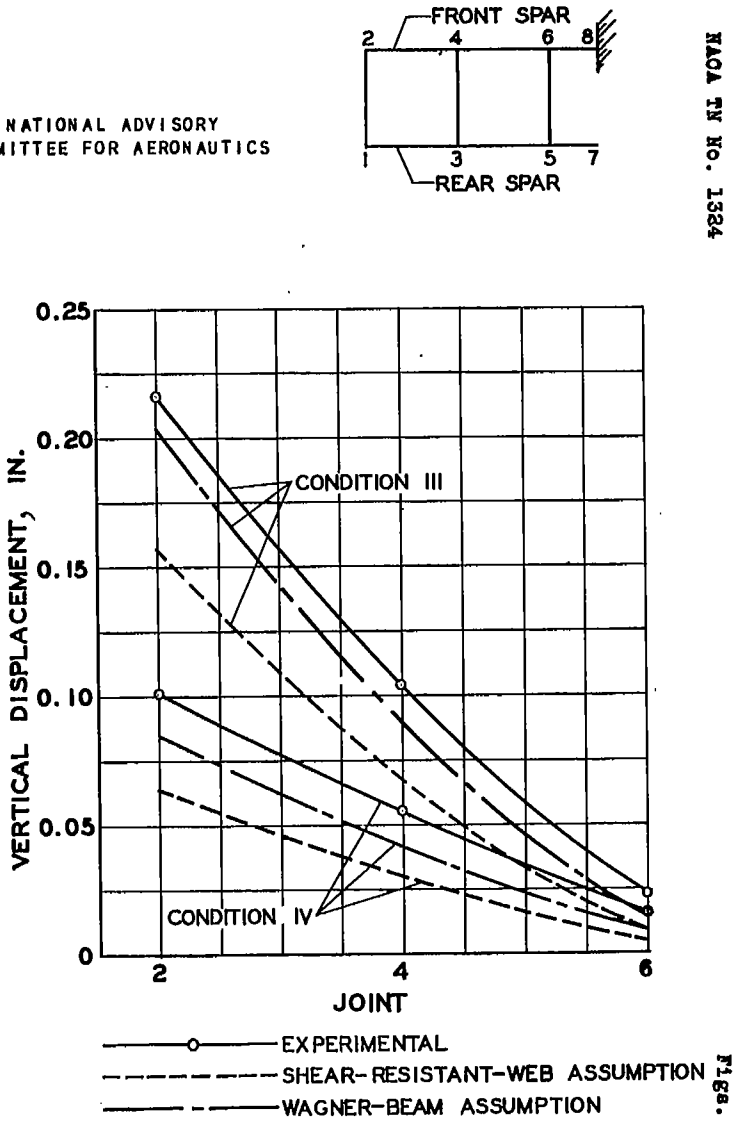


Figure 18.- Experimental and theoretical vertical displacements, front spar. Conditions III and IV; load, 150 pounds.

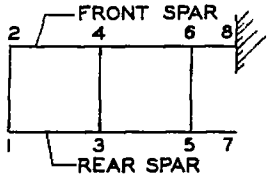


NATIONAL ADVISORY
COMMITTEE FOR AERONAUTICS

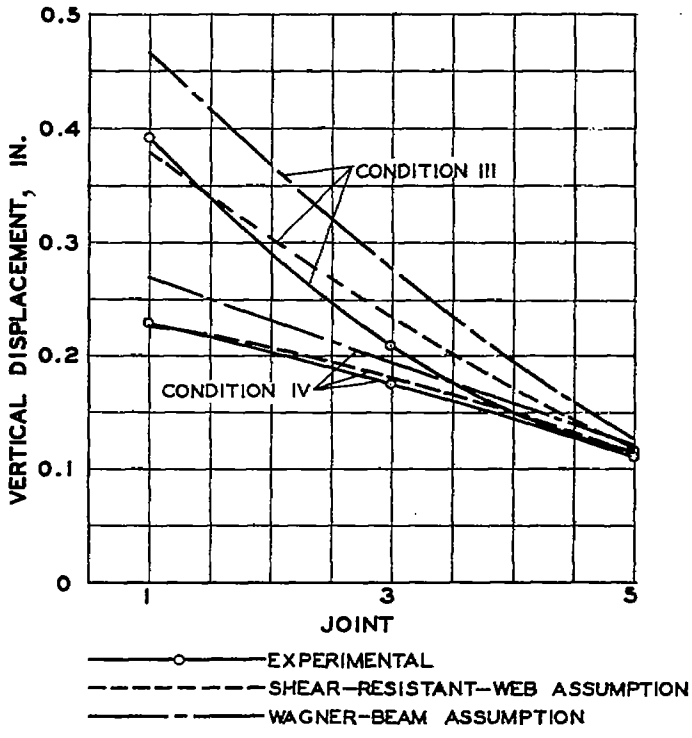


Figure 19.- Experimental and theoretical vertical displacements, rear spar. Conditions III and IV; load, 150 pounds.

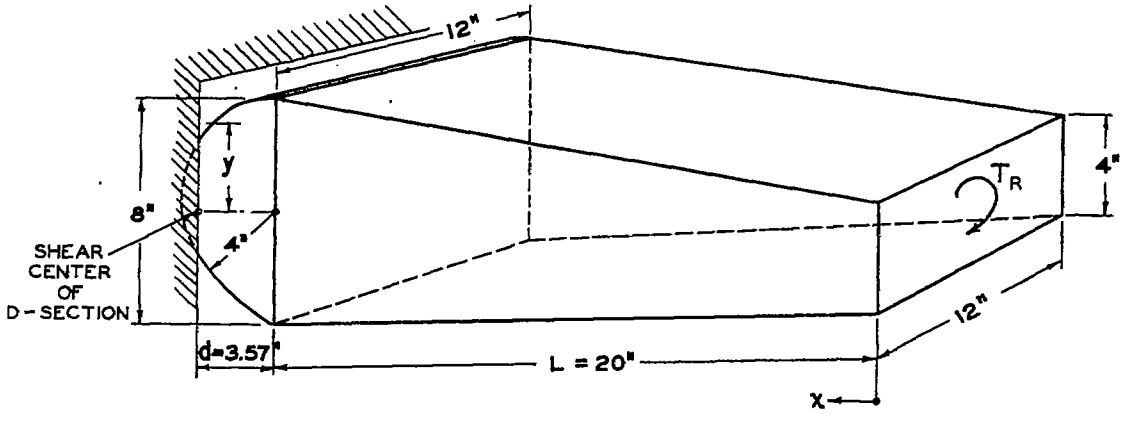


Figure 20.- Sketch of interspar member. (For assumption of shear-resistant web.)

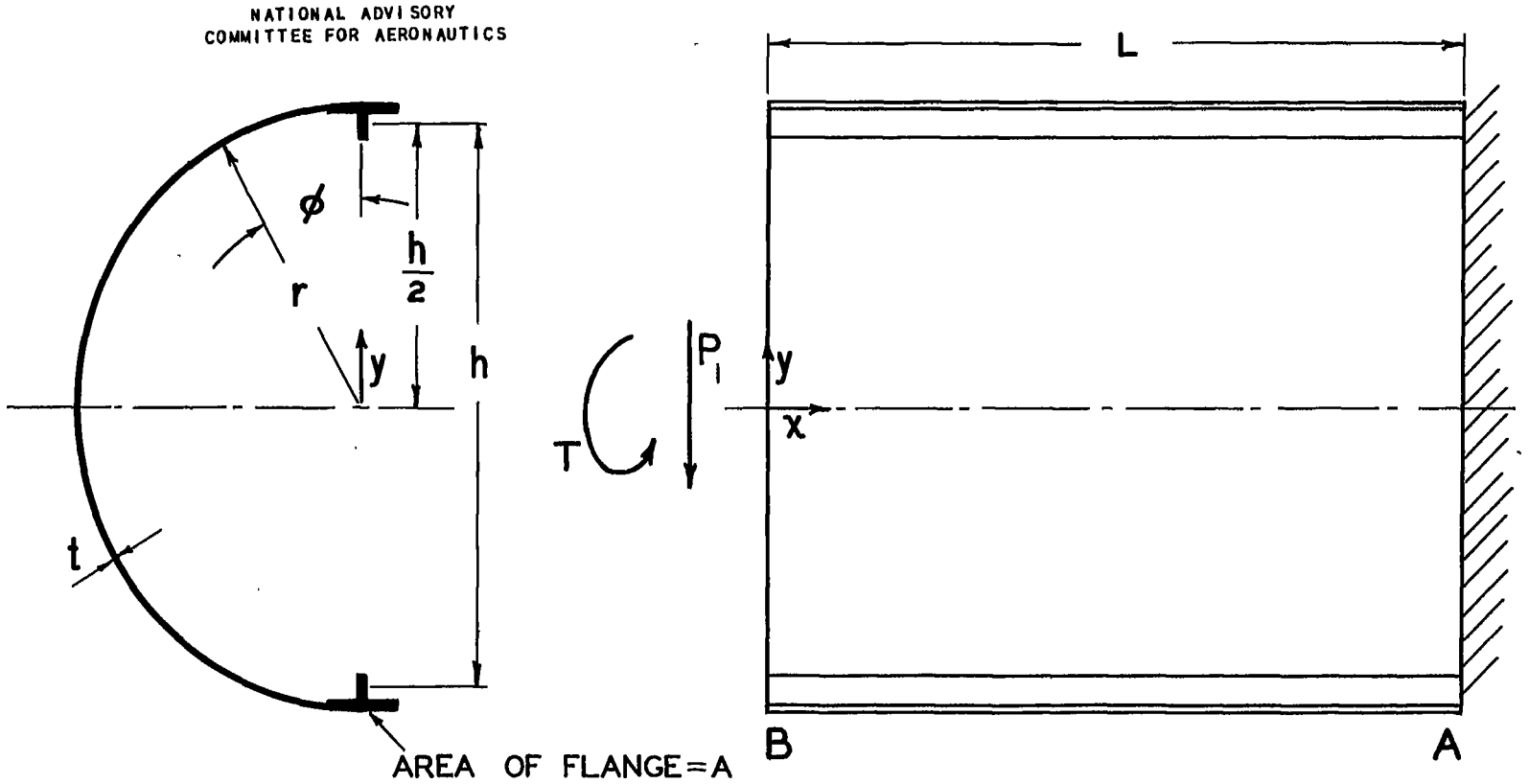


Figure 21.- Curved sheet and flanges of D-shape front spar.
(Vertical loads and displacements as well as moments and rotations are positive as shown.)